Chapter III
Localization Algorithms and Strategies for Wireless Sensor Networks: Monitoring and Surveillance Techniques for Target Tracking

Ferit Ozan Akgul
CWINS, Worcester Polytechnic Institute, USA

Mohammad Heidari
CWINS, Worcester Polytechnic Institute, USA

Nayef Alsindi
CWINS, Worcester Polytechnic Institute, USA

Kaveh Pahlavan
CWINS, Worcester Polytechnic Institute, USA

ABSTRACT

This chapter discusses localization in WSNs specifically focusing on the physical limitations imposed by the wireless channel. Location awareness and different methods for localization are discussed. Particular attention is given to indoor TOA based ranging and positioning systems. Various aspects of WSN localization are addressed and performance results for cooperative schemes are presented.

INTRODUCTION

Wireless sensor networks are ideal candidates for data gathering and remote sensing purposes in various environments, where the communications between the sensors mostly take place in a distributed

manner (Akyildiz et al., 2002). Data obtained by individual sensors are relayed to a central station for further processing and logging. Usually, information obtained through a sensor needs to be associated with the location of each sensor which necessitates the localization of sensors within certain accuracy (Patwari et al., 2005). Since primary purpose of sensor networks is to gather information on environmental changes such as temperature, pressure or humidity, it is almost always required to determine the coordinates of a specific sensor so that the appropriate steps can be taken in a more effective way in the case of emergencies. As a matter of fact, about 13.3% of the recent scientific WSN publications focus on target tracking and localization aspects as mentioned by Sohraby et al. (2007).

Owing to their small form factor and low-power consumption, WSNs have found numerous applications in both civil and military use. In the civil domain, applications can be further divided into various categories like environmental, health related, commercial and public safety applications. Environmental applications may include fire/flood detection/prevention (Pathan et al., 2006), crop quality detection, field surveying; health related applications may be listed as patient/doctor/instrument tracking inside hospitals, elderly care and remote monitoring of biological data (Cypher et al., 2006); commercial applications might be inventory control, product tracking in warehouses (Rohrig & Spieker, 2008) and remote product quality assessment. For military applications, the use of WSNs is also important in rough terrain conditions where a centralized communication system may be too costly to build (Merrill et al., 2003). Soldier and mine tracking, as well as intelligence gathering can be some applications in this domain.

As it can be seen from a sample of applications in each field, location and tracking capability is an important aspect of WSNs that need to be considered and developed further. A number of researchers studied positioning using sensor nodes and investigated the performance of algorithms and presented theoretical bounds in WSNs (Bulusu et al., 2000; Niculescu et al., 2001; Savarese et al., 2001; Savvides et al., 2001; Doherty et al., 2001; Chang & Sahai, 2004; Kanaan et al., (2006a, 2006c)). The positioning capability can be implemented using different sensing technologies like ultrasonic waves as in the Active Bat system proposed by Ward et al. (1997) or using RF or both as in the Cricket system (Priyantha et al., 2000). By using sound waves, researchers have been able to obtain cm. accuracy; however, these systems are only suitable for very small areas like a single office environment and are not intended for outdoor or indoor/outdoor hybrid node localization. In the latter case, RF solutions are generally preferred since quick deployment is possible and hardware and various ranging/localization algorithms that can be directly applied are widely available. Nevertheless, due to the nature of RF propagation, ranging/localization accuracy is not on par with solutions using sound waves. Later in this chapter we will cover the basics of RF channel and how it affects the performance of localization in various environments.

Figure 1 shows a typical setup for a WSN with location capability. Here, the sensor nodes are able to communicate with each other as well as pre-deployed anchor nodes whose coordinates are known in advance. At this point, it might be appropriate to present the two methods of WSN localization. Sensor node localization can take place in a centralized or a distributed manner.

In centralized localization, individual sensors relay their ranging estimates from the anchors to a central processing station where the localization algorithm is implemented. In the centralized approach, the processing station has the knowledge of each location requesting node and hence network topology can easily be associated with the geographical positions of the sensor nodes. Drawbacks of this method include traffic congestion and computational complexities, especially for larger sensor networks.

In distributed positioning, the sensors get ranging estimates from the anchors and try to localize themselves. After they have performed localization they might act as pseudo-anchors so that other nodes

Figure 1. Typical WSN setup

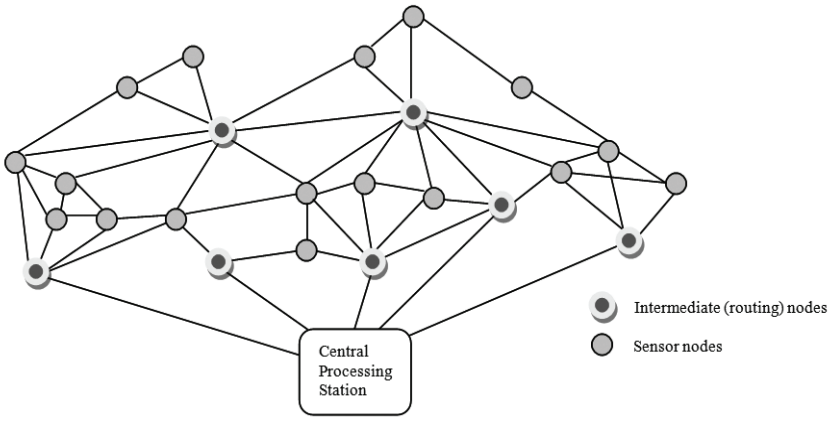

might benefit from these nodes for their own position fixing. Most of the time, pseudo-anchors will have estimation quality based on how many anchors they captured during localization and link quality for each individual anchor connection (Kanaan, 2006b). The estimation quality might be used in order to inform the end user of the overall quality factor of a particular node position. Distributed localization is most suited for large networks where central processing might be a limiting factor for the application being considered and when efficient energy utilization is required.

The performance of localization for WSNs depends mostly on the availability and quality of individual links between sensors and the anchors. The geographical distribution of the nodes with respect to each other also plays an important role in positioning accuracy. As the *connectivity* of a WSN increases, more reliable estimates can be obtained. The connectivity may be considered as a measure of how robust the WSN against node failures is. The number of alternative routes for relaying information from a specific node to the destination is directly proportional to connectivity. A high node density, as described by nodes per unit area, would primarily lead to high connectivity since nodes will be able to detect RF signals from their neighbors. On the other hand, if the nodes are sparsely connected, connectivity will be less hence nodes might not be able to obtain accurate position fixes due to lack of ranging information. Hence a high node density will provide better localization performance. A detailed analysis will be presented relating the node density to localization performance as well as performance bounds for the cooperative localization.

The overall organization of the chapter is as follows: The second section gives an overview of location awareness and a typical localization system. The third section presents the distance/position estimation metrics along with their achievable performance bounds and also the mapping techniques. Also part of this section is a brief overview of dynamic tracking and monitoring. The fourth section focuses on the TOA based ranging and localization and the challenges associated with it. The fifth section introduces and discusses the methods that can be used in the absence of DP conditions, particularly non-direct-path exploitation and cooperative localization. The sixth section presents the two studies showing the effect of various parameters on WSN localization. The seventh presents the practical implementation issues related to the implementation of WSN localization and finally the eighth section provides a conclusion for the chapter.

LOCATION AWARENESS

The question "where" might seem simple at first but the answer might not. Throughout the centuries, mankind has always tried to find the right answer to this question in his quest for exploring new lands and navigating the unknown seas. The first sailors relied on particular water currents, landmarks and positions of the celestial bodies to navigate through the waters. With the discovery of compass about 700 years ago, mariners were able to identify their directions. However, the need to get precise position and navigation, primarily for military reasons, led the nations and researchers to develop systems closer to achieving this goal. After the first developments in radio navigation starting in the first half of the 20th century (Schroer, 2003), the first successful implementation of such a system came in the form of a global positioning system or GPS, developed by the US military. In its 40 years of development and maturity, GPS has become a reliable location finding and tracking system for use not only by military but also by civilian world. Today, after various advancements in the field such as differential-GPS (DGPS) and Wide Area Augmentation System (WAAS) typical commercial grade GPS receivers can achieve accuracies of 1-5m with DGPS and 3 meters with WAAS. Study by Blomenhofer et. al (1994) reports DGPS accuracies in the centimeter range. Higher end geodetic and surveying GPS units using carrier phase, dual frequency methods and sophisticated algorithms can achieve centimeter and even sub-centimeter accuracy through GPS ambiguity resolution techniques (Kim & Langley, 2000; Poling & Zatezalo, 2002). Following GPS, other countries also started their own satellite positioning projects (EU's Galileo and Russia's GLONASS (Zaidi & Suddle, 2006)). Owing to its accurate positioning capability, most industries rely on GPS and the position information obtained via GPS (such as anchor node position information) serves as reference for other small scale localization systems.

Although GPS is a proven and reliable technology, it falls short of expectations for some terrestrial applications where the GPS signals cannot be detected due to obstructions. Satellite signals are attenuated heavily through the atmosphere and further obstruction by trees, heavy fog or manmade structures such as building tops prevent this system to be useful especially for densely populated urban settlements and inside buildings. In order to overcome this issue, researchers turned their attention to land-based positioning and tracking systems for situations that cannot make use of satellite signals.

After the proliferation of cellular based radio communications systems, FCC mandated mobile phones be located within a certain accuracy (FCC, 1999). According to this report, mobile operators should be able to locate phones with 50m accuracy 67% of the time and 150m accuracy 95% of the time for handset based positioning, and 100m accuracy 67% of the time and 300m 95% of the time for network based positioning.

The fundamentals of locating and tracking RF emitting devices differ greatly from those of data communications. In communications, information is transferred from one entity to another and the information carrier might be RF, sound or light. A single link, as long as it is reliable, will be enough to transfer data between the entities. However, locating a device whose location is completely unknown requires a completely different approach than transmitting data.

Localization might be realized in two ways:

- Geometric methods (Trilateration, triangulation, hyperbolic methods)
- Fingerprinting methods (Signal mapping)

Geometric methods include techniques that can locate or track devices based on signal properties that are estimated. TOA/TDOA, RSS and AOA are examples of geometric measurement techniques.

Fingerprinting methods require a two-phase approach. In the first phase (also called the off-line phase), a database is formed based on signal parameters and this database is utilized in the second phase to estimate the location. Nearest-neighbor mapping and artificial neural networks are examples of such methods (Dasarathy, 1991; Heidari et al., 2007b; Nerguizian et al., 2006; Kanaan & Pahlavan, 2004a).

Overview of a Localization System

A typical localization system consists of mobile terminals (nodes in case of a WSN) that need to be located/tracked, beacon or anchors serving as reference points, a central processing station that implements the positioning algorithm and keeps track of all the terminals as well coordinates data communications and a higher layer system that shows the results of positioning or tracking like an LCD panel. Figure 2 shows the components of such a localization system. The system might use different ranging metrics for obtaining the position information. The most common of these metrics are RSS, TOA/TDOA and AOA. RSS and TOA might be considered as ranging metrics since ranging information can be obtained from these signal parameters. The nodes will need at least three ranging estimates from different anchors to be able to obtain a position fix. In the case of AOA, two different AOA estimates from two anchors will suffice to obtain a location fix. More details will be given for each of these techniques in the coming sections.

DISTANCE/POSITION ESTIMATION METRICS

As mentioned in the previous section, a localization system needs to obtain range estimates from fixed anchors or reference points in order to estimate the location of a node. Ranges estimates can be obtained using different metrics. RSS and TOA/TDOA are examples of such techniques.

RSS: After the RF signal is transmitted by a transmitter, its energy experiences loss that is proportional to the distance signal travels. A common model based on single-path radio propagation is given by

Figure 2. High level architecture of a typical positioning system

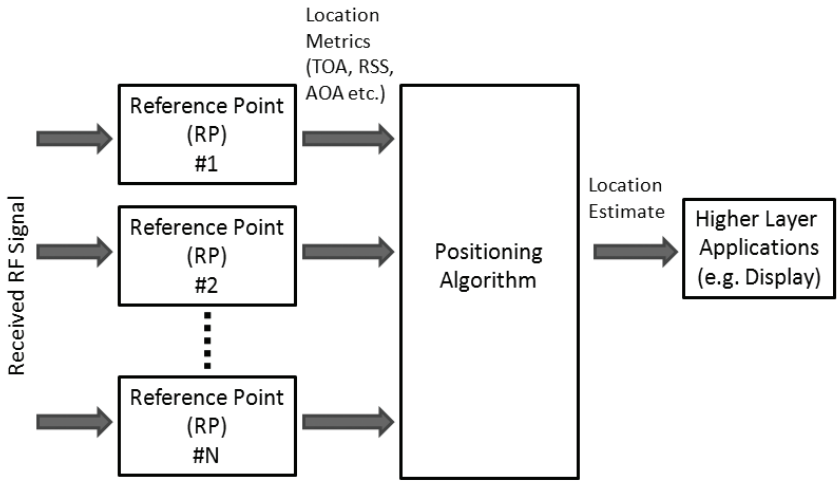

$$P_r(dB) = P_t(dB) - 10\alpha \log_{10} d \tag{1}$$

where P_r (dB) and P_t (dB) denote the received and transmitted signal powers in dB. α is the distance-power gradient and is dependent on the propagation environment. For free space, $\alpha = 2$. A wide range of values are possible for α, i.e. for a brick construction office environment α is reported to be 3.9 or for a laboratory environment with metal-faced partitioning it is found to be 6.5 (Pahlavan & Levesque, 2005).

Other empirical models have also been developed based on extensive measurements in various environments. Motley (1988) proposed a path-loss model for multi-floor buildings. Technical working group of TIA/ANSI JTC recommended an indoor path loss model (JTC, 1994) for PCS applications. Apart from the indoor model, the same group proposed micro and macro-cellular models for outdoor applications. Other popular models for outdoor environments are the Okumura (1968), Hata (1980) and COST231 (1991) models.

Either by using the simple radio-propagation or the more complicated empirical models, distance information can be obtained from the received signal power given the transmitted signal power. Although this method can be easily applied since almost all RF wireless devices can report received signal strength, its accuracy is not always acceptable due to the stochastic variation of the channel. The path loss models discussed in this section are deterministic models that do not consider the fading and shadowing effects. At any time instant, the signal level experiences slow and fast fading caused by local scatterers and the movement of the receiver node. Slow fading is also called Shadow fading and it is generally modeled as a zero-mean normal variable, *X(dB),* in the logarithmic scale. Hence shadows are generally log-normally distributed. The probability density function (pdf) for the log-normal distribution is given as:

$$f(x) = \frac{1}{x\sigma\sqrt{2\pi}} e^{-\frac{(\ln(x)-\mu)^2}{2\sigma^2}} \tag{2}$$

where μ and σ are the mean and standard deviation respectively.

Hence the received power can be given as

$$P_r(dB) = P_t(dB) - 10\alpha \log_{10} d + X \tag{3}$$

Due to this fluctuating behavior of received signal power, accurate ranging measurements are not always possible hence leading to lower accuracy position estimation. In fact, the accuracy of such estimation is lower bounded by its Cramer-Rao lower bound (CRLB). CRLB basically specifies the lower bound on the variance of estimation. For the simplistic RSS model this bound has been given by Qi and Kobayashi (2003) as:

$$\sigma_{RSS} \geq \frac{(\ln 10)}{10} \frac{\sigma_{sh}}{\alpha} d \tag{4}$$

Here, σ_{RSS} is the standard deviation of RSS estimation, σ_{sh} is the variance for shadow fading, d is the actual distance between the transmitter and the receiver and α is the power-distance gradient.

AOA: AOA information from two different anchors might be used to determine the position of a node by using triangulation as shown in Figure 3. AOA estimation is also referred to as direction-of-arrival (DOA) estimation, direction finding or bearing estimation in many contexts and has been researched

Figure 3. Triangulation of a node by two anchors

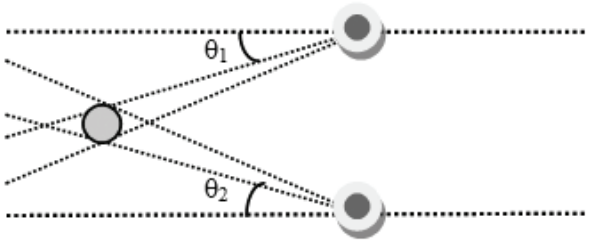

extensively in the literature (Cedervall & Moses, 1997; Krim & Viberg, 1996; Kumaresan & Tufts, 1983; Li et al., 1995; Stoica & Sharman, 1990; Tewfik & Hong, 1992). A common method for AOA estimation is by using special structures called uniform linear arrays (ULA) (Schelkunoff, 1943). The n elements of an ULA with spacing d can be used to estimate the direction of arrival of a RF signal based on the following relation:

$$\theta = \arcsin\left(\frac{c\Delta t}{d}\right) \tag{5}$$

where θ is the angle at which the signal is impinging upon the ULA, c is the speed of light, Δt is the time difference between the arrivals of the signal at consecutive array elements and d is the spacing between consecutive elements.

To achieve finer results by using a certain antenna array configuration one can employ super-resolution techniques. Although various methods are available in literature, most common ones are MUSIC (Schmidt, 1986) and ESPRIT (Roy & Kailath, 1989) and their variations (Rao & Hari, 1989; Ottersten et al., 1991). Kuchar et al. (2002) report angular estimation variance of 1º with 0dB SNR and down to 0.01º with SNRs of about 40 dB.

The performance bounds for AOA estimation can also be studied to derive the CRLB. The bound for AOA is formulated to be (Tingley, 2000)

$$\sigma_{AOA} \geq \frac{c\sqrt{2}\sqrt{BN_0}}{N\Delta 2\pi f_c \sin(\theta) A A_T} \tag{6}$$

where σ_{AOA} is the standard deviation for AOA estimation, c is the speed of light, B is the bandwidth of the signal, N_0 is the noise spectral density, N is the number of elements of the ULA, Δ is the spacing between the elements, A is the channel coefficient. A_T and f_c are respectively the amplitude and carrier frequency of the source signal $x(t)$ denoted as

$$x(t) = A_T \cos 2\pi f_c t \tag{7}$$

The *SNR* of the signal can be expressed as

$$SNR = \frac{A^2 {A_T}^2}{BN_0} \tag{8}$$

so we can rewrite (6) as

$$\sigma_{AOA} \geq \frac{c\sqrt{2}}{N\Delta 2\pi f_c \sin(\theta)\sqrt{SNR}} \tag{9}$$

From (9), it can be seen that the CRLB is inversely proportional to the number of elements N, f_c and SNR. Thus having a high SNR and high frequency signal like an Ultra-Wide-Band (UWB) signal as well as a high number of array elements give higher resolution AOA estimation. Oppermann et al., 2004 give an overview of UWB signals and their applications.

TOA: Another distance estimation method is the TOA method in which the range is estimated based on the time the signal spends traveling from the transmitter to the receiver. Since the speed of RF propagation is very well known in both free space and air, it gives a direct estimation of the distance between the transmitter and the receiver once the travel time is estimated. When TOA systems are considered, the only important parameter that needs to be estimated correctly in a multipath propagation environment is the TOA of the LOS path or the direct-path (DP). Other multipath components are not important for ranging and localization purposes except for the cases when the DP is not available. This condition will be investigated in detail in the section *Challenges for the TOA based Systems.* The basic equation needed to obtain the distance is given as

$$d = \tau_{DP} c \tag{10}$$

where d is the distance estimate, τ_{DP} is the TOA of the DP and c is the speed of light. Accurate TOA estimation needs perfect synchronization between the clocks of the transmitter and the receiver. Clock synchronization might be achieved by regular data exchange between the transmitter and the receiver or an additional anchor for correcting the clock bias. Although 3 anchors are necessary to obtain position, a 4th anchor will be needed for time correction. This method is readily applied for the GPS in which a 4th satellite is used to compensate for the receiver clock bias. The TOA location estimation is depicted

Figure 4. Trilateration of a node by three anchors (RSS and TOA)

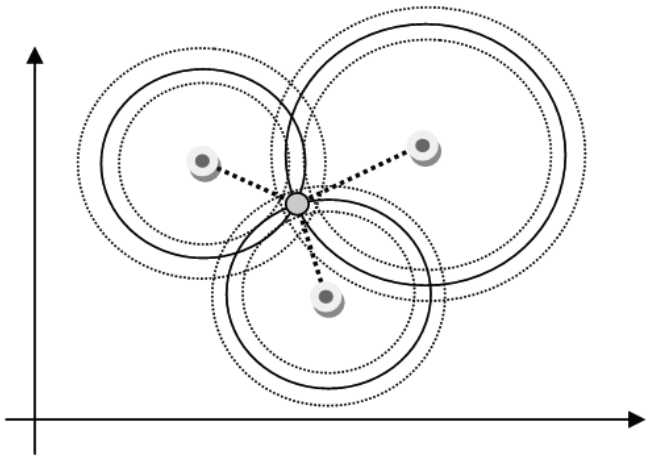

in Figure 4 where a perfect synchronization is assumed between the transmitters and the receiver. Same procedure also applies to the RSS method in which individual distance estimates are also used for position fixing. The dotted circles denote the uncertainty in range estimation hence leading to an area for the possible location of the receiver between the three estimation circles, rather than a single point.

Several methods are available to estimate the TOA. The traditional methods of estimation are the inverse Fourier transform (IFT) and maximum-likelihood (ML) estimations. The latter one is also called the cross-correlation method.

In the IFT method, observed frequency domain channel response is transformed into time-domain to obtain the time-response of the channel (Figure 5). The delay value of the DP is then used to calculate the distance.

The ML method assumes the following signal model for the estimation of TOA (Li, 2003).

$$r(t) = s(t-\tau) + w(t) \tag{11}$$

Here r(t) is the received signal, s(t) is the transmitted signal, τ is the delay and w(t) is noise modeled as AWGN. The signal at the receiver is basically a delayed version of the signal plus noise. ML dictates that maximum possible cross-correlation of the transmitted and the received signal occurs at the actual delay of the signal shown as (Li, 2003; Knapp & Carter, 1976)

$$\frac{d}{d\tau}\left(\int_{T_0} r(t)s(t-\tau)dt\right)\Bigg|_{\tau=\hat{D}_{ML}} = 0 \tag{12}$$

To obtain the delay estimate, τ is varied over a range of delay values and the value of τ that gives the maximum of the cross-correlation (or equivalently makes the derivative of the cross-correlation equal to 0) becomes the distance estimate. A block diagram is also given in Figure 6 to show the implementation of this method.

In the case of single path TOA estimation as applied to (11), CRLB is computed to be

$$\sigma_{\hat{D}}^2 \geq \frac{1}{8\pi^2}\frac{1}{SNR}\frac{1}{BT_0}\frac{1}{f_0^2 + B^2/12} \tag{13}$$

where $\sigma_{\hat{D}}^2$ is the variance of TOA estimate, $B = f_2 - f_1$, $f_0 = (f_2 + f_1)/2$ and T_0 is the observation time. From (13), it is easy to see that the bound is inversely proportional to the SNR, the signal bandwidth and observation time.

Figure 5. IFT operation for obtaining CIR

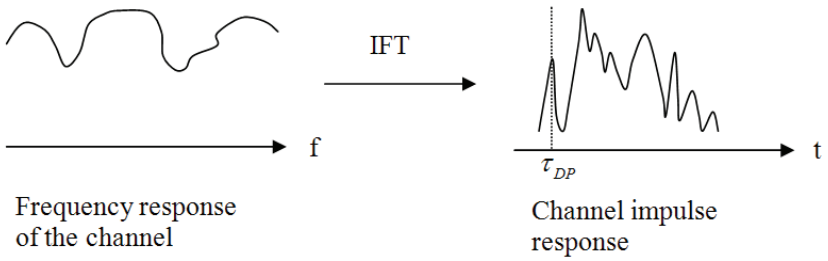

Figure 6. ML TOA estimation (reproduced from (Li, 2003))

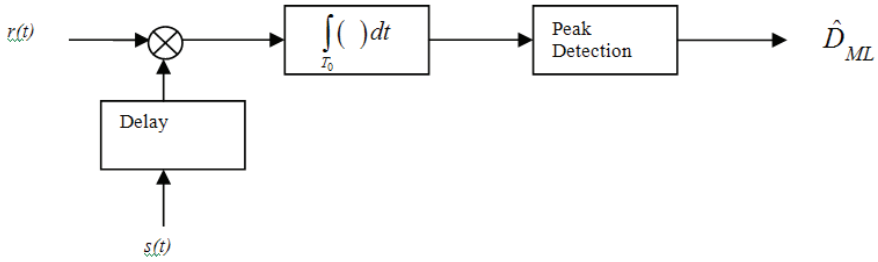

Figure 7. Hyperbolic positioning of a node by three anchors (TDOA)

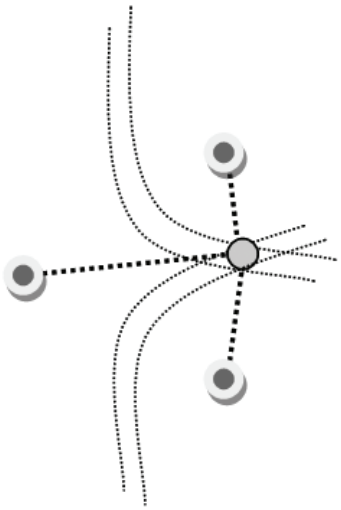

Similar to the AOA case, super-resolution methods might be used to extract indistinguishable peaks from the channel response in time-domain. This method has been shown to be effective in both wide-band and narrow band TOA estimation methods (Li & Pahlavan, 2004; Dumont et al., 1994) making these methods superior to traditional ML and cross-correlation methods.

TDOA: TDOA, also known as hyperbolic positioning, is a method whereby the receiver calculates the differences in the TOAs from different RPs. By using this method the clock biases between the transmitters and receivers are automatically removed, since only the differences between the TOAs from two transmitters are only considered. The estimation using TDOA is shown in Figure 7.

Mapping Techniques

Fingerprinting or mapping techniques are also widely studied for their robustness in terms of performance and some advantages in comparison to geometric methods. The fingerprinting methods employ a two-step approach. The first step involves the construction of the signal map for a desired environment (also called the offline phase), the second step is the actual positioning step (online phase). These techniques

inherently capture all environment related propagation effects like multipath, shadowing, scattering etc and hence might be used for applications where geometric methods fall short of expectations. However due to extensive measurement and mapping involved in this approach, it might not be preferred for large areas where it may not be feasible. Additionally the structural changes in the environment might necessitate remapping for the affected regions of the database (Bahl & Padmanabhan, 2000; Nerguizian et al., 2006; Steiner et al., 2008). The two most commonly used mapping methods are the RSS mapping and CIR mapping. In RSS mapping, a receiver terminal is taken to almost every feasible part of an area that is intended to be mapped and signal power from multiple anchors are recorded into the database. Once mapping is done, actual positioning is obtained by comparing the RSS in online phase to one of the mapped points. The algorithms employed for this purpose are mostly k-NN algorithms (Dasarathy, 1991; Hatami & Pahlavan, 2005). Another application is the mapping of CIR for desired locations. The unique characteristics of the CIR, such as rms delay spread, average power… etc might then be used for comparison (Heidari et al., 2007b; Nerguizian et al., 2006). The same paper also discusses the use of neural networks for position estimation.

Overall Comparison for Different Localization Methods

Geometric Methods	**Advantages**	**Disadvantages**
RSS	- Simple to implement (most wireless devices report power) - Not sensitive to timing and RF bandwidth	- Not accurate - Requires models specific to application case and environment
AOA	- Only requires 2 anchors for localization	- DP blockage and multipath affects accuracy - Requires use of antenna arrays/smart antennas - Accuracy is dependent on RF bandwidth
TOA/TDOA	- Accurate ranging/localization can be obtained - Can be scaled to a multitude of applications	- Accuracy is dependent on RF bandwidth - DP blockage might cause large errors
Mapping Methods	- Captures all channel related parameters hence resilient to DP blockage	- Requires extensive database construction/training

Tracking and Dynamic Monitoring

Most of the time, the nodes to be located are mobile and hence it becomes essential to determine the location of these mobile nodes periodically. This real-time periodic location update is also called "tracking". Tracking keeps a history of the location information and hence is considered as a dynamic methodology for the localization problem. As opposed to blind positioning, which is based either on geometric or fingerprinting method and which basically requires locating the node without any prior position information, tracking makes use of location history to estimate the future positions. This might be obtained by various methods. The most popular of these approaches is to employ a Kalman Filter (Kalman, 1960), which is a recursive filter that estimates the state of a system in the presence of noisy measurements. However, for most systems that do not exhibit linear behavior, Kalman filtering is not an effective solution. For these non-linear systems other types of filtering such as Extended Kalman Filtering (EKF) (Haykin, 2002) and Unscented Kalman Filtering (UKF) (Julier & Uhlmann, 1997) are preferred. EKF is particularly useful for nonlinear but differentiable systems. It is a first order approximation for the nonlinear filtering problem. UKF, on the other hand is applicable to highly nonlinear systems and produces more accurate results than EKF. Another advantage of UKF over EKF is that

UKF does not require the computation of Jacobians that are needed for EKF. Hence it is more practical from an implementation point of view.

Another method is to use dead reckoning (Beauregard, 2006; Randell et al., 2003) which estimates the future position based on current speed, bearing and elapsed time. Inertial navigation systems are based on this principle. Even though these systems might obtain estimates for incomplete measurements, error propagation is a major concern for prolonged duration of information absence. Hence these tracking methods should be complemented with other true positioning approaches for a more complete positioning system design.

TOA-BASED RANGING AND LOCALIZATION

Due to recent advances in UWB signaling and hardware and its potential for accurate ranging, TOA based ranging systems utilizing UWB signals have gained particular popularity (Lee & Scholtz, 2002; Gezici et al., 2005; Qi et al.; 2004). On the other hand, the knowledge gained by the implementation and challenges of the now widely used GPS system has been instrumental in the advancement of these TOA systems. The following parts of this section will particularly focus on the TOA-based systems.

Peak Detection Strategies for TOA Based Systems

In this part, we present the two most commonly used methods for obtaining ranging measurements, which have also been outlined by Denis et al. (2003). In the following, τ_{sel} denotes the estimated TOA.

Detection of the First Peak

This method relies on the detection of the first available peak in the CIR. As long as the first path power is above the detection threshold of the system, the method gives the best possible results for ranging. However, accurate detection depends on high SNR (mostly DDP conditions) which is not always possible. The path decision can be expressed as

$$\tau_{sel} = \{\tau_i \mid i = \arg\min_p \tau_p\} \tag{14}$$

where τ_p is the TOA for the pth path.

Detection of the Strongest Peak

In this method, the path with the strongest power is detected and its TOA is considered as the ranging estimate between the transmitter and the receiver. Detecting the strongest peak is easily implementable when compared with the first method; however ranging accuracy is not always acceptable since the strongest path may not always be the DP. Most practical receivers implementing this method are S-rake receivers (Oppermann et al., 2004). Path decision in this case is

$$\tau_{sel} = \{\tau_i \mid i = \arg\max_p P_p\} \tag{15}$$

where P_p is the power of the pth path.

Challenges for the TOA-Based Systems

One major challenge facing the high precision TOA systems is the obstruction of the DP in the channel profile. Since the DP is the true indicator of the range between the transmitter and the receiver, its obstruction by various means such as metallic or thick concrete walls will lead to substantial ranging errors. This particular obstruction of the DP leads to a specific channel impairment that has been named as the undetected direct path (UDP) condition (Pahlavan et al., 1998; Wylie & Holtzman, 1996). To understand the effects of DP obstruction, it is convenient to consider the commonly used mathematical expression for channel impulse response at this point. This model takes into account the multipath components (MPCs) that arrive at the receiver via different propagation mechanisms such as reflection, transmission or scattering and is given as:

$$h(\tau, t) = \sum_{i=1}^{L} \beta_i \delta(t - \tau_i) e^{j\phi_i} \tag{16}$$

where h denotes the CIR, L is the number of MPCs, β_i is the gain(amplitude), τ_i is the TOA and φ_i is the angle (phase) of the i^{th} arriving path respectively. The DP might be characterized as the path having gain β_1, TOA τ_1 and phase φ_1. In this case the range between the receiver and the transmitter will be

$$d = \tau_1 c \tag{17}$$

When the DP is blocked or cannot be detected, the indirect paths will be detected giving rise to substantial ranging errors. Figure 8 and Figure 9 below, show real world example channel profiles for both DDP and UDP obtained using a 1GHz bandwidth UWB signal. In the DDP case there is only 50cm of ranging error that can be attributed to the limited bandwidth (multipath error) of the signal, whereas the UDP case (by inserting a metallic shield in between the transmitter and receiver) introduces more than 2m of ranging error for the same setup.

Figure 8. Sample DDP channel profile

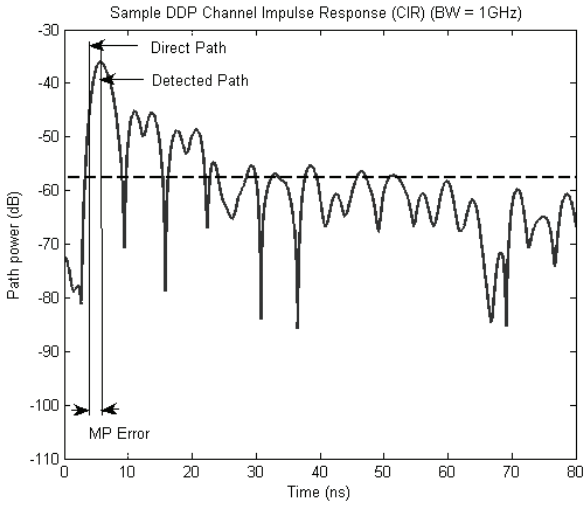

Figure 9. Sample UDP channel profile

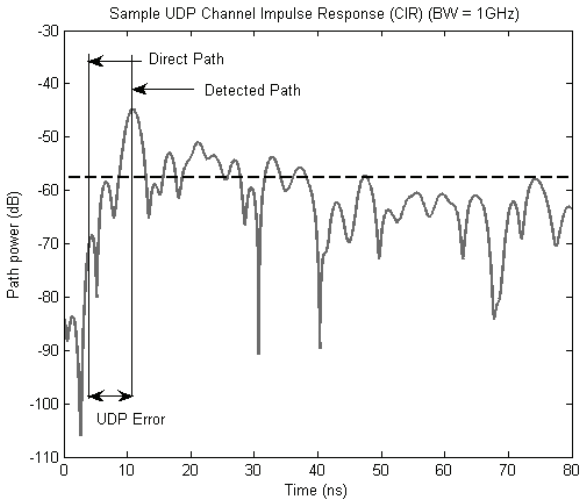

Next, we will present a new study on the detection of UDP conditions. The method presented here tries to estimate the occurrence of UDP condition hence necessary actions might be taken to mitigate the errors associated with UDP regions by employing proper adjustments to ranging data.

UDP Identification

Another open problem in the field of localization and positioning is the problem of identification of the channel profiles which exhibit unexpected large ranging errors. In traditional localization the distance measurements from different RPs were incorporated into the localization algorithm without mitigating the effects of ranging error. Therefore, the accuracy of the localization system would degrade drastically when problem of UDP occurred. This part investigates different techniques for identification of these channel profiles (UDP identification) with large ranging errors. We have used propagation parameters of the wireless channel and observed channel profile at the receiver side to decide whether a channel profile is in UDP conditions (Heidari et al., (2007a, 2007b)). To illustrate the effectiveness of such identification of channel profiles with UDP conditions, we set up an experiment with very limited number of RPs and compared the performance of the traditional algorithm with the proposed algorithm based on UDP identification. In the proposed algorithm we suggest to adjust the value of the distance measurement once a channel profile is identified to be in UDP conditions. The adjustment is performed by subtracting a correction value from the distance measurement (Heidari et al., (2007a, 2007b)). The amount of the correction value is determined based on predefined distributions of the ranging error in the typical environments similar to the building under study.

As discussed in the previous sections, the most important and distinguishing parameter in TOA-based localization system is the presence of the DP component. Detecting the DP component results in accurate ranging estimate of the true distance between the antenna pair. On the other hand, the erroneous estimation of the distance of the antenna pair results in large ranging error observed by the localization system and drastically degrades the performance of such systems. Therefore, we face two hypotheses:

$$\begin{cases} H_0 : DDP \mid d_{FDP} \approx d_{DP}, \varepsilon \approx 0 \\ H_1 : UDP \mid d_{FDP} \gg d_{DP}, \varepsilon \gg 0 \end{cases} \tag{18}$$

where H_0 denotes the DDP hypothesis, which indicates that the channel profile can effectively be used for localization, and H_1 denotes the UDP hypothesis, which indicates that the channel profile is not appropriate for being used for localization purposes.

There are two types of metrics being extracted from channel profile which can be utilized in identification of UDP conditions. The first class of metrics, is the time delay characteristics of the channel profile, while the second class deals with power characteristics of the channel profile. We can also utilize a hybrid metric, consists of time and power, in order to classify the receiver location.

Time Metrics

Delay information encrypted in the channel profile is our first time metric to investigate. Amongst all of the delay metrics the mean excess delay of the channel profile is the easiest to find and perhaps the most effective metric, relatively, to efficiently identify the UDP conditions. We used a Ray-Tracing (RT) database for modeling the different distributions of mean excess delay in this section. Mean excess delay is defined as the

$$\tau_m = \frac{\sum_{i=1}^{L_p} \hat{\tau}_i \left|\alpha_i\right|^2}{\sum_{i=1}^{L_p} \left|\alpha_i\right|^2} \tag{19}$$

where $\hat{\tau}_i$ and α_i represent the TOA and complex amplitude of the i^{th} detected path, respectively, and L_p represents the number of detected peaks. Conceptually, it can be observed that profiles with higher mean excess delay are more likely to be UDP conditions.

Power Metrics

RSS is a simple metric that can be measured easily and it is measured and reported by most wireless devices. For example, the MAC layer of IEEE 802.11 WLAN standard provides RSS information from all active access points (APs) in a quasi-periodic beacon signal that can be used as a metric for localization (Kanaan et al., 2006b)

$$-P_{tot} = r = 10\log_{10}\left(\sum_{i=1}^{L_p} \left|\alpha_i\right|^2\right) \tag{20}$$

For identification, we used $r = -P_{tot}$ which is referred to as power loss. It can be observed that profiles with higher power loss are more likely to be UDP conditions.

Hybrid Time/Power Metric

Although, each time or power metric can be used individually to identify the class of receiver locations, but one can form a hybrid metric to achieve better results in identification of the UDP conditions. Here,

we propose to use a hybrid metric consisting of TOA of DP component and its respective power as the metric to identify the UDP conditions. Mathematically

$$\zeta_{hyb} = -P_{FDP}\tau_{FDP} \tag{21}$$

where ζ_{hyb} represents the metric being extracted. It can be shown that the desired metric can be best modeled with Weibull distribution.

Binary Hypothesis Testing

Knowledge of the statistics of τ_m, r, and ζ_{hyb} enables us to identify the UDP conditions. In order to do so binary likelihood ratio tests can be performed to select the most probable hypothesis (Heidari et al., 2007a). For this purpose, we picked a random profile and extracted its respective metrics. The likelihood function of observed RMS delay spread,τ_{mi}, for DDP condition can then be described as

$$L(H_0 \mid \tau_{m_i}) = \mathrm{P_r}(\tau_{m_i} \mid H_0) \tag{22}$$

Similarly, the likelihood function of observed mean excess delay, τ_{mi}, for UDP condition can be described as

$$L(H_1 \mid \tau_{m_i}) = \mathrm{P_r}(\tau_{m_i} \mid H_1) \tag{23}$$

The likelihood ratio function of τ_m can then be determined as

$$\Lambda(\tau_{m_i}) = \frac{\sup\left\{L(H_0 \mid \tau_{m_i})\right\}}{\sup\left\{L(H_1 \mid \tau_{m_i})\right\}} \tag{24}$$

The defined likelihood ratio functions are the simplified Bayesian alternative to the traditional hypothesis testing. The outcome of the likelihood ratio functions can be compared to a certain threshold, i.e. unity for binary hypothesis testing, to make a decision

$$\Lambda(\tau_{m_i}) \underset{H_1}{\overset{H_0}{\gtrless}} \eta_\tau \tag{25}$$

Similar procedure takes place to obtain the other likelihood ratio functions. Each of the above likelihood ratio tests can individually be applied for UDP identification of an observed channel profile. The outcome of the likelihood ratio test being greater than unity indicates that the receiver location is more likely to be a DDP condition and can appropriately be used in localization algorithm while the outcome less than unity indicates that the profile is, indeed, more likely to belong to UDP class of receive location; hence, the estimated d_{FDP} has to be remedied before being used in the localization algorithm.

To use the likelihood functions more effectively, we can combine the functions and form a joint likelihood function. Using the distributions obtained from RT database for UDP identification we can exploit τ_m,r and ζ_{hyb} distributions and their respective parameters obtained from RT channel profiles to form the joint density function. Assumption of the independence of the likelihood functions leads to a suboptimal combined likelihood function defined as

$$\Lambda(\tau_m, r, \zeta_{hyb}) = \Lambda(\tau_m)\Lambda(r)\Lambda(\zeta_{hyb}) \quad (26)$$

For the simulation of the accuracy of the UDP identification we set up a small experiment that consisted all the RT channel profiles existing in our database. We used channel profiles, including the ones used for obtaining the parameters, for UDP identification and recorded the percentage of accuracy of each method. The results of the accuracy of the likelihood hypothesis tests, individually and as a joint distribution, are summarized in Table 1.

It can be observed that the accuracy of using individual metrics for identification of UDP conditions is about 70% while combining the metrics for UDP identification can achieve 90% of accuracy.

LOCALIZATION AND TRACKING IN THE ABSENCE OF DIRECT PATH

The previous part introduced the concept of UDP condition and its effect on the TOA estimation problem. Furthermore, a study describing the identification of UDP has also been given in order to predict the occurrence of such conditions in order to mitigate the errors associated with it. In this part we will focus on methods that try to alleviate the UDP problem by the exploitation of indirect paths in regions of UDP and the concept of cooperative localization for a WSN.

Exploiting Non-Direct Paths

The existence and detectability of DP is essential for accurate ranging estimates in TOA based systems as stated earlier. However, since the availability of DP cannot be guaranteed for typical indoor localization systems, other alternatives should be considered to improve ranging accuracy. One of them is to exploit the multipath components in the channel.

Multipath components might be used to remedy UDP conditions if they exhibit steady behavior in the region of interest. Figure 10 illustrates the basic principle underlying the relationship between the TOA of the direct path and a path reflected from a wall, for a simple two path scenario. As the mobile receiver moves along the *x*-axis, the change in the distance in that direction is related to the length of the DP by $dx\cos\alpha = dl_{DP}$. As the geometry of the shows, for the reflected path we also have $dx\cos\beta = dl_{P_n}$. Therefore, we can calculate the change in the length of the direct path from the change in the reflected path, using

$$dl_{DP} = dl_{P_n}\frac{\cos\alpha}{\cos\beta} \quad \text{or} \quad d(TOA_{DP}) = d(TOA_{P_n})\frac{\cos\alpha}{\cos\beta} \quad (27)$$

Table 1. Accuracy of the likelihood hypothesis test

Likelihood Ratio	*Correct Decision*
τ_m	70.85 %
r	67.06 %
ζ_{hyb}	69.73 %
$\Lambda(\tau_m, r, \zeta_{hyb})$	89.29 %

In other words, knowing the angle, β, between the arriving path and direction of movement and the angle, α, between the direction of movement and the DP, we can estimate the changes in the TOA of the DP from changes in the TOA of the reflected path. A study based on this principle is introduced by Akgul & Pahlavan (2007).

In order to use a path other than the DP for tracking the location, we should be able to identify that path among all other paths, and the number of reflections for that path should remain the same in the region of interest. In the simple two path model shown in Figure 10, the second path consistently reflects from one wall as we move along the region and hence we can identify that path easily because it is the only path other than the DP. Since both conditions hold for the second path, the behavior of the TOA of that path, shown in Figure 10-b, is smooth and we can use it for tracing the DP. In realistic indoor scenarios, in the absence of direct path, we have numerous other paths to use and the simplest paths to track are the first detected path (FDP) and the strongest path (SP).

With regard to channel behavior, we need to look into the principles underlying this behavior to learn how to remedy the situation. The basic problem is path-indexing changes, and the rate of path indexing exchange is a function of number of paths in the impulse response. The number of paths can be reduced by restricting the AOA of the received signal using a sectored antenna. Using sectored antennas to restrict the AOA provides two benefits: (I) it reduces the number of multipath components and hence reduces the path index crossing rate, facilitating improved tracking of specific paths in the channel profile; (II) it allows a means for estimating the angle of the arriving path needed in (27). Figure 11 shows the behavior of the SP at a receiver using sectored antenna with a variety of aperture angles. Details of this setup have been outlined by Pahlavan et al., 2006.

Figure 11 shows the ideal behavior of different paths without bandwidth considerations as a receiver moves along the left segment of the rectangular route. The blue line shows the actual distance and the blue line with star marker shows the behavior of the FDP, which in this case is also the strongest path. The receiver starts in a DDP condition, then moves to a UDP region, and then returns to another DDP area. In the DDP regions the DP, FDP and the SP are the same and the range estimate is accurate and consistent (steady). In the UDP region, the FDP, which is also the SP, remains steady for short periods but due to the path index changes of the FDP it cannot maintain its steadiness and it experiences about ten transitions of the path index or reflection scenario for the FDP. This high rate of transitions is due

Figure 10. (a) Basic two path reflection environment; (b) Relation between the TOA of multipath and DP

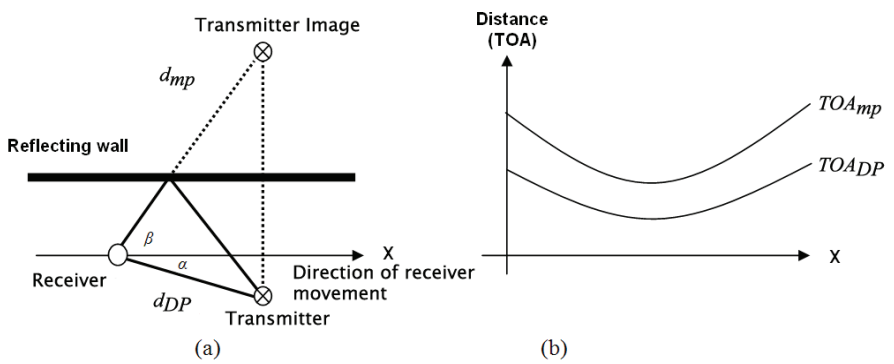

Figure 11. UDP region

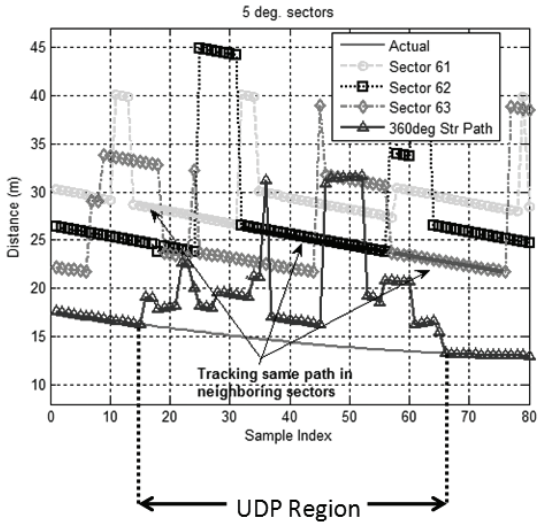

to the large number of multipath components and we can reduce these components by using sectored antennas to limit the AOA of the paths.

Figure 11 also shows the behavior of the SP in three neighboring 5 degree sectors along a UDP region. These are three of the 72 ideal 5 degree sectors assumed in this example. The SP at the start of the UDP region is in sector 61, and then it moves to sectors 62 and 63. As the SP moves among these sectors it has a steady behavior with no change in path index, which we can use for the detection of the TOA of the DP.

The discussion above shows the potential for the implementation of ranging using non-direct paths with an ideal sectored antenna with 5 degrees aperture angle for each sector and a simple algorithm which traces the strongest path as it moves from one sector to the next neighboring sector. Development of more practical algorithms to implement this concept with finite bandwidth and realistic antennas will require significant additional research.

Cooperative Localization

Background

The previous sections have provided an understanding of the different traditional approaches to the localization problem. It is evident that the localization accuracy depends on the ranging metric, deployment environment (which affects the ranging error statistics), and the relative geometry of the sensor node to the anchors. The major difference between traditional localization and WSN localization is cooperative localization. Cooperative localization refers to the collaboration between sensor nodes to estimate their location information. In traditional wireless networks, nodes can only range to specific anchors. As a result, nodes that are beyond the coverage of sufficient anchors fail to obtain a location estimate. In a cooperate WSN, however, nodes do not need to have a single-hop connection to anchors in order to localize. Cooperative localization makes propagating range information throughout the net-

work possible. Due to random deployment in a WSN, some parts of the network may still be isolated or may not have the required number of connections to nearby nodes (hence ill-connected), which further introduces limitations in position estimation. Obviously, increasing the sensor node density can reduce the probability of isolated sub-networks, but this approach has its own limitations. With increased range information cooperative localization has the following advantages: The first is that the *coverage* of the anchor nodes to the sensor nodes increases substantially compared the traditional counterpart. Second, the increased range information between the nodes allows for improvements in localization accuracy.

In two-dimensional localization we need at least three links or connections to reference terminals with known locations. These links may have different qualities of estimate for the distance between the reference and target terminals, depending on the availability of direct path in the channel. In cooperative precise localization in multipath-rich environments, we simply avoid ranging estimates reported from the links with UDP conditions. In other words the redundant information provided by the additional reference points is used to reduce the localization error. This situation is common in ad-hoc and sensor networks where we have a fixed infrastructure of known reference points for positioning and a number of mobile users in the area. When we want to locate a mobile terminal, in addition to the distances from the respective fixed reference points, we can also use the relative distances from other mobile users. We refer to this approach as cooperative localization since the localization is conducted through a cooperative method. A similar approach is also used for general localization in sensor and ad-hoc network when we have a limited number of dispersed references and a number of ad-hoc sensor terminals with less than an adequate number of connections to reference points (Savares et al., 2001; Savvides et al., 2005). For general localization, we only need the whereabouts of the terminals and the literature in that field does not address the large error caused by UDP conditions. The concept introduced in this part uses the redundancy of the links embedded in the sensor and ad-hoc network environments to achieve precise indoor localization.

Figure 12 shows a positioning scenario with three reference transmitters in a selected office building and a loop-route scenario. The transmitter TX-1 located in a large laboratory on the left side of the building has UDP conditions caused by the RF-isolation chamber in 40% of locations around the loop, transmitter TX-2 located in the small office on upper parts of the building layout, covers the entire loop without any UDP location, and transmitter TX-3 located in the lower corridor has around 50% UDP conditions around the loop caused by the elevator. The route estimation-1 in Figure 12 shows the results of location estimation using the traditional least square algorithm (Pahlavan et al., 2006) with the three known reference transmitters along the loop. Whenever the direct path is present, for example in the lower and right hand routes, the DME is small. As we have one or two UDP conditions for our three links to the references, for example in the upper route, the DME is substantially large. This observation suggests that whenever direct path is available for all links we can achieve precise localization, but as soon as one of the links loses the direct path we have large localization errors. In other words, if we avoid UDP conditions we can achieve precise positioning. Therefore, if we have more than the minimum number of references, assuming we can detect the UDP conditions, we can avoid links with UDP and achieve precise localization. A method of UDP detection and identification will also be presented at the end of this chapter.

To demonstrate the effectiveness of this approach, we consider an example where we have two other RPs, transmitter TX-4 and transmitter TX-5, which are located in good positions, where each has three direct path connections to the main reference transmitters. As shown in Figure 12, when we use the three main reference transmitters to estimate the location of transmitter TX-4 and transmitter TX-5 we

Figure 12. Cooperative localization

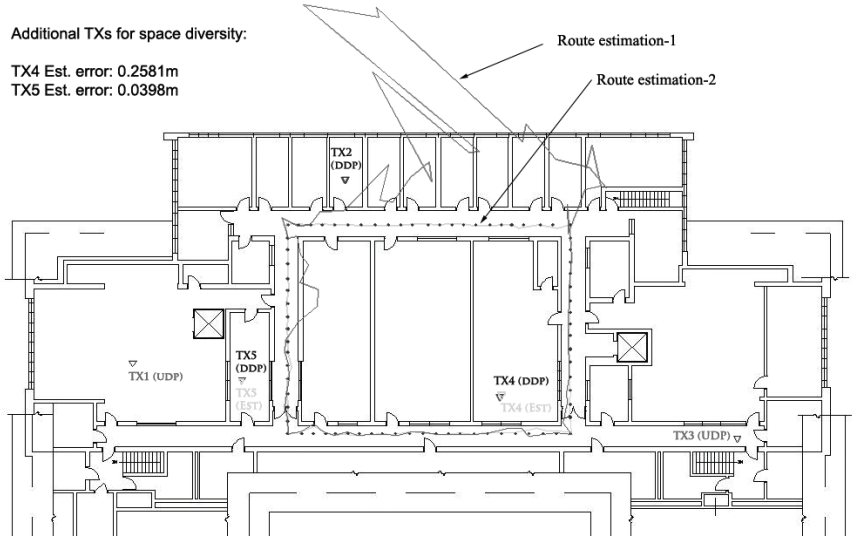

have very good estimated locations for them. In an ad-hoc sensor environment we can assume that our target receiver moving along the loop route can also measure its distances from transmitter TX-4 and transmitter TX-5. In this particular example, as shown in the figure, these ranging estimates are also very accurate because they are based on the availability of the direct path. The route estimation-2 in Figure 12 shows the estimate of location for the mobile terminal as it moves along the loop when it uses the estimated locations of transmitter TX-4 and transmitter TX-5 and the actual location of transmitter TX-2 to locate itself with the traditional least squares algorithm. As shown in Figure 12, our estimates are now substantially more accurate. The drastic improvement in the accuracy of localization is a result of avoiding UDP conditions and taking advantage of the redundancy of the ad-hoc sensor networks to achieve precise cooperative localization.

In the above example, we showed the potential advantage of using the redundancy in sensor and ad-hoc networks to achieve precise cooperative positioning. In practice, we need to develop algorithms for implementation of this concept. These algorithms need the intelligence to discover the quality of ranging estimates and possibly occurrence of the UDP conditions to use them for positioning. The algorithms for general cooperative localization first suggested in (Savares et al., 2001) and later on discussed in the follow up literature (Gezici et al., 2005; Savvides et al., 2005) are not applicable to our approach. We need new algorithms to address specific methods to handle the behavior of the DME errors in the absence of direct path, which is reported by Alavi and Pahlavan (2006). We have to find techniques for relating a quality of estimate to each ranging and positioning estimate in order to develop precise cooperative localization algorithms for sensor and ad-hoc networks. These algorithms should take advantage of redundancy to avoid unreliable reference sources and achieve robust precise localization. More research in this area is needed for the design of algorithms that take account of different radio propagation conditions.

Challenges Facing WSN Localization Algorithms

The major challenges facing WSN localization can be categorized into network and channel parameters. When considering network parameters, localization is usually constrained by the size (i.e., the number of nodes and *anchors*), the topology, and the connectivity of the network. Anchors or *beacons* are sensor nodes that are aware of their locations (usually through GPS or pre-programmed during setup) and they are necessary for WSN applications that require localization with respect to an absolute global frame of reference, e.g., GPS. Network connectivity is determined by node density, which is usually defined as the number of nodes in a meter square (nodes/m^2). A network with a high node density exhibits improved localization performance compared to a sparse network. A study related to localization performance vs. node density will be presented after this section. Furthermore, in sparse WSNs there is a high probability of ill-connected or isolated nodes and in such cases localization accuracy can be degraded substantially. Therefore, it is always favorable to increase the node density (higher connectivity information means a lower probability of ill-connected networks) to improve the accuracy of localization. However, with increased sensor nodes, the error propagates and accumulates from one hop to the next, which can be a serious problem in WSN localization algorithms. Error propagation in WSN localization is the accumulation of errors in estimated sensor node positions in each iterative step. When a node *transforms* into an anchor, the error in the range estimates used in the localization process impacts its position estimate. When other nodes in the network use this newly transformed anchor, the position error will *propagate* to the new node. Therefore, in several iterative steps, error propagation can substantially degrade the localization performance. Finally, the topology and geometric relation between nodes will further add limitations to the localization performance.

The second and most limiting factor affecting WSN localization is the wireless RF channel. Effective cooperative localization hinges on the RF ranging technology and its behavior in the deployed environment. For example, deploying hundreds of nodes in outdoor environments faces different challenges as opposed to trying to locate sensors inside a building. WSNs in indoor areas, particularly, face severe multipath fading and harsh radio propagation environments, which causes large ranging estimation errors that impact localization performance directly. To develop practical and accurate cooperative localization algorithms, the behavior of the wireless channel must be investigated and incorporated. Specifically, the localization algorithms used to determine the position must be able to assess the quality of the ranging estimates and integrate that information into the localization process.

Performance

The performance of WSN localization algorithms can be determined through very well established CRLB analysis that has recently attracted attention from different scholars and researchers. The definitions of the bound and thus the analytical derivation involved are similar, but they usually differ in their assumptions about the characteristics of the corrupting noise. The details of these different approaches for computing the CRLB are beyond the scope of the chapter and the interested reader can find more details in (Larsson, 2004; Savvides et al., 2005; Chang & Sahai, 2006). Due to its simplicity and applicability to sensor networks, we now provide an overview of CRLB analysis provided by Savvides et al. (2005) for unbiased estimate of the sensor positions. Although this is not the case in certain environments, such as indoors, it provides, nonetheless, a very important analytical foundation for analyzing the localization performance in WSNs.

For known anchor locations $\boldsymbol{\varphi} = [x_{N+1},\ldots,x_{N+M},y_{N+1},\ldots,y_{N+M}]^T$, we wish to estimate the unknown locations of sensor nodes, $\boldsymbol{\theta} = [x_1,\ldots,x_N,y_1,\ldots,y_N]^T$. The CRLB provides a lower bound on the error covariance matrix for an unbiased estimate of è (Savvides et al., 2005). For a given estimate of the sensor locations $\hat{\boldsymbol{\theta}}$ and Gaussian range measurement noise *z*, the Fisher Information Matrix (FIM) can be represented by (Savvides et al. 2005)

$$J(\boldsymbol{\theta}) = E\left\{\left[\nabla_{\boldsymbol{\theta}} \ln f_z(Z;\boldsymbol{\theta})\right]\left[\nabla_{\boldsymbol{\theta}} \ln f_z(Z;\boldsymbol{\theta})\right]^T\right\} \tag{28}$$

where $f_z(Z;\boldsymbol{\theta})$ is the joint Gaussian PDF given by

$$f_z(Z;\boldsymbol{\theta}) = \frac{1}{(2\pi)^K |\Sigma|^{\frac{1}{2}}} \exp\left\{-\frac{1}{2}\left[z-\mu(\boldsymbol{\theta})\right]^T \Sigma^{-1}\left[z-\mu(\boldsymbol{\theta})\right]\right\} \tag{29}$$

where $\mu(\boldsymbol{\theta})$ is the vector of the actual distances between the sensor nodes corresponding to available *K* measurements. FIM for the specific PDF in can be written as

$$J(\boldsymbol{\theta}) = \left[G(\boldsymbol{\theta})\right]^T \Sigma^{-1}\left[G(\boldsymbol{\theta})\right] \tag{30}$$

where $G(\boldsymbol{\theta})$ contains the partial derivatives of $\mu(\boldsymbol{\theta})$. The CRLB is then given by

$$CRLB = \left[J(\boldsymbol{\theta})\right]^{-1} \tag{31}$$

More detailed implementation of the CRLB expression can be found in Savvides et al. (2005).

WSN algorithms should then compare the localization performance to the widely available CRLB analysis in literature. One important note here is that both the bound and the algorithm performance rely mainly on the statistics of the ranging error. Although sensor density and geometry have an impact on the performance, the statistics of the ranging error specifically provides the main challenge for accurate localization. If the ranging error assumptions taken into the algorithm and the CRLB analysis do not reflect the actual behavior of the propagation channel, both the algorithm performance and the bound will be non-realistic. For the indoor ranging scenarios where range estimates are not just corrupted by zero mean Gaussian noise (a positive bias can corrupt the TOA measurements) we will need to analyze CRLB for biased estimates. In the presence of such biases, the Generalized-CRLB (G-CRLB) can be obtained instead and it has been derived for traditional wireless networks by Van Trees (1968) and for indoor WSNs by Qi et al. (2006). A detailed treatment of this problem is available by Alsindi & Pahlavan (2008).

A STUDY OF RP DENSITY AND MSE PROFILING ON WSN LOCALIZATION

In this section, we will be investigating the effects of various parameters that are related to localization in sensor networking.

In the first part, we will be showing how RP density affects the localization performance by using two different localization algorithms.

Effects of RP Density on TOA-Based UWB Indoor Positioning Systems

The performance of UWB indoor positioning systems based on TOA techniques is generally affected by the density of RPs, as well as UDP conditions. For a fixed number of RPs, the performance of some indoor positioning algorithms tends to degrade as the size of the area is increased, i.e. the RP density is decreased. In this part, we evaluate the effects of RP density on the performance of different positioning algorithms in the presence of empirical distance measurement error (DME) models derived from UWB measurements in typical indoor environments. We then present functional relationships between RP density and positioning mean-square error (MSE) for these algorithms. These relationships can be used for more effective indoor positioning system design and deployment. Finally, we investigate the effects of bandwidth with respect to improving the performance of these algorithms.

In addition to the inherent stochastic variations of the channel (which can induce distance measurement error, or DME), the indoor environment itself also does not necessarily stay static. Indoor areas can be remodeled, made larger, or portions of it can be rebuilt with different building materials. This will change the RP density and by extension, the estimation accuracy that we can obtain from the network used for positioning. The RP density, denoted by ρ, can be viewed as a measure of the number of RPs per unit area, and is defined as:

$$\rho = N / A \tag{32}$$

where N is the number of RPs covering a given indoor area, and A is the size of the area, generally given in m^2. It is noted in a prior work by Kanaan and Pahlavan (2004b) that given a *fixed* number of RPs, the performance of certain positioning algorithms tends to degrade as the size of the area to be covered is increased (i.e the RP density is decreased). This observation makes intuitive sense since the DP will be attenuated more as the distance between the RP and the sensor is increased. This will give rise to more DME which, in turn, will lead to degraded location estimation performance. Although the effects of RP density on location estimation accuracy has been known, the exact nature of the functional relationship between these two quantities has not, to the best of our knowledge, been formulated to date. This raises a valid question: why is it important to characterize this relationship? The answer fundamentally lies in the fact that different indoor positioning applications have different requirements for estimation accuracy. For example, in a commercial application (such as inventory tracking in a warehouse), low accuracy might be acceptable. However, in a public-safety or military application (such as keeping track of the locations of firefighters or soldiers within a building), much higher accuracy would be needed. This implies that the RP densities required for these two application domains would be different. Knowledge of the functional relationship between RP density and estimation accuracy enables a system designer to figure out how many RPs are required to meet a given accuracy target, thereby results in a cost-effective network deployment.

The manner in which RP density affects positioning accuracy depends principally on two factors: the particular algorithm used for the location estimation, and the DME model. The basic contribution of this paper is to explore these kinds of relationships for different positioning algorithms, both to get an insight into their performance, and also to provide a useful tool for designers of indoor positioning networks. In addition to addressing the above-mentioned issues, this part also extends the study reported by Kanaan and Pahlavan (2004b) in two important ways. First, the performance evaluations we undertake are based on DME models obtained from empirical UWB measurements in a typical indoor

area, rather than models derived from ray-tracing simulations. Second, since the DME also depends on bandwidth (Alavi & Pahlavan, 2003), we also explore the impact of bandwidth on the performance of a given algorithm.

The relationship between RP density and positioning accuracy has been studied, mainly for ad-hoc sensor networks. Savarese et al. (2001) have studied positioning in distributed ad-hoc sensor networks through cooperative ranging. The paper by Chintalapudi et al. (2004) studies the effects of density of RPs on ad-hoc positioning algorithms employing both distance and bearing measurements. While these works have identified the relationship between positioning accuracy and RP density, they have not explicitly presented that relationship mathematically. Also, the DME models used in these studies are generally very simple. Here, we seek to explore the functional dependency of the positioning accuracy (as expressed by the *mean square error* or *MSE*) on RP density in the presence of DME models based on empirical measurements within actual indoor environments.

UDP conditions generally occur in cases where there are multiple walls and/or metallic objects between the transmitter and the receiver. As a result, the DP can experience severe fading (Pahlavan et al., 2002). It has also been observed that UDP conditions tend to occur along coverage boundaries or areas with coverage deficiencies (Alavi et al., 2005). As mentioned above, UDP occurs only on occasion and when it does, it is the dominant source of error for distance measurements. However, the DDP error is always present. Based on extensive UWB measurements, a DME model is introduced by Alavi et al. (2005). The model is given by:

$$\hat{d}_i = \begin{cases} d_i + \xi_{DDP,w} \log(1+d_i) & \text{DDP case} \\ d_i + \xi_{DDP,w} \log(1+d_i) + \xi_{UDP,w} & \text{UDP case} \end{cases} \tag{33}$$

where $\hat{d}_i$ is the observed distance measurement from the i-th RP, and $\xi_{DDP,w}$ and $\xi_{UDP,w}$ are random variables that characterize the DDP and UDP-based DME respectively. The distributions of $\xi_{DDP,w}$ and $\xi_{UDP,w}$ have been observed to be Gaussian and dependent on bandwidth, i.e, $\xi_{DDP,w} = N(m_{DDP,w}; \sigma^2_{DDP,w})$ and $\xi_{UDP,w} = N(m_{UDP,w}; \sigma^2_{UDP,w})$ where the means (denoted by $m_{DDP,w}$ for $\xi_{DDP,w}$ and $m_{UDP,w}$ for $\xi_{UDP,w}$) and standard deviations (denoted by $\sigma^2_{DDP,w}$ for $\xi_{DDP,w}$ and $\sigma^2_{UDP,w}$ for $\xi_{UDP,w}$) are a function of the system bandwidth, w, used to make the TOA-based distance measurements (hence the subscript w). The parameters for the distributions, as a function of the bandwidth w, are listed in Table 2.

Additionally, it has been determined through measurements that the probability of UDP occurrence $P_{UDP,w}$ increases as the bandwidth is increased (Alavi et al., (2005). Observations indicate that $P_{UDP,w}$ values also depend on the actual distance between the transmitter and the receiver. Specifically,

$$P_{UDP,w} = \begin{cases} P_{UDP\_close,w} & d \le 10\text{m} \\ P_{UDP\_far,w} & \text{otherwise} \end{cases} \tag{34}$$

The error modeling introduced here is detailed by Alavi et al. (2005). This model can be compared to the work by Alavi & Pahlavan (2003) and has a fundamentally different approach. Alavi & Pahlavan's model (2003) was developed based on Ray-Tracing results and categorized the conditions of the channel as Line-of-sight / Obstructed line-of-sight (LOS/OLOS), assuming that in the OLOS case, we always have the UDP case. However, the introduced DME model is based on UWB measurement data and classification of the channel as DDP and UDP, as this approach reflects the behavior of the indoor channel in a more realistic manner.

Table 2. Parameters for DDP and UDP-based DME

w(MHz)	500	1000	2000	3000
$m_{DDP,w}$ *(m)*	0.21	0.09	0.02	0.004
$\sigma_{DDP,w}$ *(cm)*	26.9	13.6	5.2	4.5
$m_{UDP,w}$ *(m)*	1.62	0.96	0.76	0.88
$\sigma_{DDP,w}$ *(cm)*	80.87	60.45	71.53	152.21
$P_{UDP\_far,w}$	0.33	0.62	0.74	0.77
$P_{UDP\_close,w}$	0.06	0.06	0.07	0.12

Algorithms

We investigate the effects of RP density on the performance of two algorithms using simulations: the Closest-Neighbor with TOA Grid (CN-TOAG) (Kanaan & Pahlavan, 2004a), and the Davidon LS algorithm (Davidon, 1968).

CN-TOAG Algorithm

In essence, the CN-TOAG algorithm estimates the location of the sensor S, by minimizing the following objective function:

$$f(x,y)=\sqrt{\sum_{k=1}^{N}\left(d_k-\sqrt{(x-X_k)^2+(y-Y_k)^2}\right)^2} \tag{35}$$

where $(X_k; Y_k)$ is the location of the k-th RP, dk is the observed distance measurement from the k-th RP and $(x; y)$ is the unknown location of the sensor to be estimated. The estimated location is the one that minimizes (35). In order to find the minimum, one needs to solve the following partial differential equation:

$$\left(\frac{\delta f(x,y)}{\delta x},\frac{\delta f(x,y)}{\delta y}\right)=0 \tag{36}$$

Due to the complexity of $f(x; y)$ in (35), it is not feasible to solve (36) analytically. Therefore, the CN-TOAG algorithm tries to solve it numerically using the concept of a TOA grid (Kanaan & Pahlavan, 2004a). The size of the grid, as given by the spacing between grid points, h, is a major determinant of performance for this algorithm. Specifically, values of h below a certain value can result in better performance than the LS algorithm (Kanaan & Pahlavan, 2004a).

Davidon Least-Squares Algorithm

The particular instance of the LS algorithm that has been used for our evaluations is the one by Davidon (1968), which attempts to minimize the objective function:

$$f(\mathbf{x}) = f(x, y) = \sum_{k=1}^{N} \left(d_k - \sqrt{(x - X_k)^2 + (y - Y_k)^2} \right) \tag{37}$$

in an iterative manner using the following relation:

$$\mathbf{x}_{k+1} = \mathbf{x}_k - \mathbf{H}_k g(\mathbf{x}_k) \tag{38}$$

where $\mathbf{H}_k$ represents an approximation to the inverse of the Hessian of f(x), G(x), which is defined as:

$$\mathbf{G}(\mathbf{x}) = \begin{pmatrix} \frac{\partial^2 f}{\partial x^2} & \frac{\partial^2 f}{\partial x \partial y} \\ \frac{\partial^2 f}{\partial y \partial x} & \frac{\partial^2 f}{\partial y^2} \end{pmatrix} \tag{39}$$

and g(x) is the gradient of f(x), defined as:

$$g(\mathbf{x}) = \left(\frac{\delta f(\mathbf{x})}{\delta x}, \frac{\delta f(\mathbf{x})}{\delta y} \right) \tag{40}$$

The following relation defines when the computations will be terminated:

$$\eta_k = (g(\mathbf{x}_{k+1}))^T \mathbf{H}_k (g(\mathbf{x}_{k+1})) \tag{41}$$

so that the iterations will stop when $\eta_k \leq \varepsilon$, where ε is a small tolerance value.

Simulation Platform

Figure 13 shows the general system scenario, where a regular grid arrangement of RPs is assumed to be available. The use of the regular grid arrangement for the RPs is common in indoor wireless networks, as this approach often provides adequate coverage (Unbehaun, 2002). We also note that this system scenario is a fundamental building block for certain indoor ad-hoc sensor networks, and could be a considered a realistic deployment scenario for such scenarios (Stoleru & Stankovic, 2004). The important parameter that determines performance is not the absolute number of RPs, but the ratio of the number of RPs to the area, as given by (32).

Here, we consider varying sizes of L for each algorithm. By varying the room size while keeping the number of RPs fixed at each of the four corners, we evaluate the performance of positioning algorithms as a function of RP density in the scenario and also show the effect of system bandwidth on overall performance. Synchronization mismatch between the transmitter and receiver is assumed to be small. For each algorithm, a total of 5000 uniformly distributed random sensor locations are simulated for different bandwidth values and for varying room dimensions. In line with the FCC's formal definition of UWB signal bandwidth as being equal to or more than 500 MHz (FCC, 2002), we will present our results for bandwidths of 500, 1000, 2000, and 3000 MHz. Once a sensor is randomly dropped in the

Figure 13. General system scenario

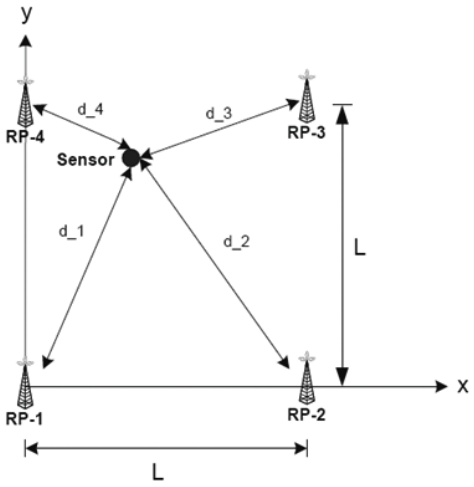

area, the actual distance measurements, d_i, from each RP at the corners are individually corrupted with DME, as given in (33). The corrupted distance measurements are then fed into the positioning algorithm to get the position estimate. As noted by Kanaan & Pahlavan (2004a), the performance of the CN-TOAG algorithm is dependent on the size of the TOA grid, as determined by the bin size, h, which for the purposes of this study, was fixed at 0.3125 m.

Results

The results are shown in Figure 14, Figure 15, and Figure 16 . From the Figure 14 and Figure 15 we can immediately see that as the node density is increased, the MSE decreases. This is an expected result, since a finer installation of the RPs will reduce the probability of the occurrence of UDP conditions and hence will result in better positioning accuracy. Another important observation is that as the bandwidth of the system is increased, the estimation accuracy is also increased with the exception of 3 GHz. Increasing the system bandwidth provides a better time resolution, thereby ensuring accurate estimation of the TOA of the DP. However, increasing the bandwidth beyond a certain point (2000 MHz in this case) also gives rise to increased probability of UDP conditions due to the faster attenuation of higher bandwidth signals. In Figure 16, we compare the performance of LS and CN-TOAG as a function of RP density using a system bandwidth of 2000 MHz. This bandwidth was arbitrarily selected, since it appears to be the bandwidth where both algorithms perform best. The results clearly indicate that CN-TOAG has better performance, particularly for higher values of ρ. Since CN-TOAG is based on the concept of a TOA grid, increasing ρ (i.e. decreasing the area) for a fixed bin size h brings the grid points closer together. This, in turn, places a much tighter bound on the positioning error for CN-TOAG. By examining the results of the simulation, we can derive a mathematical relation between RP density and MSE by applying a third order polynomial fit to the results. Our choice of the third order polynomial was simply influenced by the fact such a fit showed better agreement with simulation results than, say, a second-order fit. We have chosen to derive these relations on the basis of Monte-Carlo simulations,

Figure 14. Performance of LS algorithm

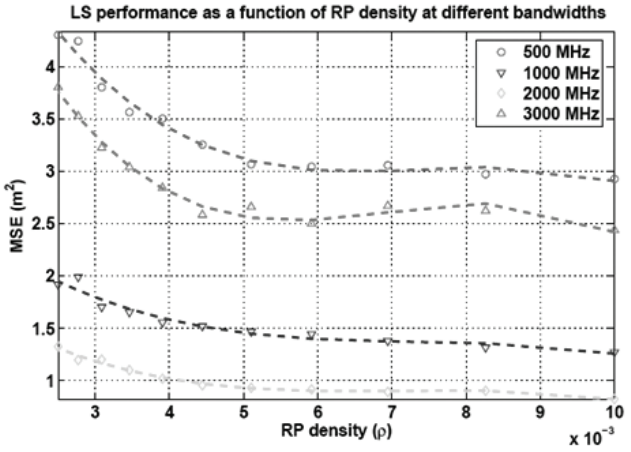

Figure 15. Performance of CN-TOAG algorithm

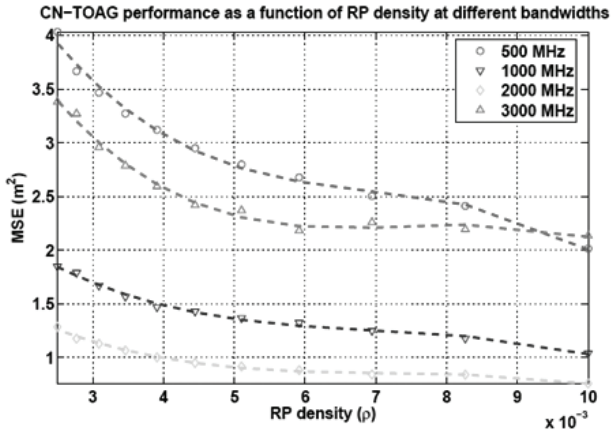

rather than analytically, in order to be able to compare and contrast the performance of the LS and CN-TOAG algorithms. It is certainly possible to derive these relations analytically for the LS algorithm, but not necessarily for CN-TOAG due to the complexity of the objective function of (35). These relations can be a valuable tool in determining the RP density for a required positioning accuracy. The 3rd order polynomial is given as:

$$MSE = a_3 \rho^3 + a_2 \rho^2 + a_1 \rho + a_0 \tag{42}$$

where a_i ($i \in \{1,2,3,4\}$) denote the polynomial coefficients. Table 3 and Table 4 show the coefficient values for the two algorithms. These values are dependent on the DME model used; however, we note that the DME model parameters are still representative of typical indoor environments. A simple numerical

Figure 16. Performance of CN-TOAG and LS for 2000 MHz

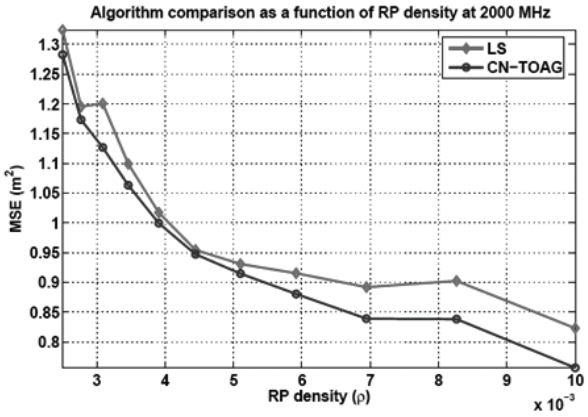

Table 3. Coefficients of the 3rd degree polynomial fit for LS algorithm

w(MHz)	a_3	a_2	a_1	a_0
500	-1.20e+07	2.69e+05	-1.98e+03	7.7776
1000	-4.53e+06	1.00e+05	-749.52	3.2647
2000	-4.36e+06	93645	-662.95	2.4484
3000	-1.72e+07	3.60e+05	-2427.4	7.8446

Table 4. Coefficients of the 3rd degree polynomial fit for CN-TOAG algorithm

w(MHz)	a_3	a_2	a_1	a_0
500	-1.15e+07	2.42e+05	-1771	7.0203
1000	-4.61e+06	97736	-725.22	3.1171
2000	-3.51e+06	76142	-557.93	2.2317
3000	-1.04e+07	2.34e+05	-1728.7	6.4152

example illustrates how these relations could be used. Suppose we have a 900 m^2 indoor area where we would like to implement a positioning system using CN-TOAG at a bandwidth of 1 GHz, and we would like the MSE to be no more than 1.5 m^2. Referring to Figure 15, we see that the corresponding value of ρ should be no less than 0.004. Using our knowledge of the size of the area, the value of ρ, and (32), we see that we need to have a minimum of 4 RPs in order to ensure satisfactory performance.

Conclusions

In this part, we have investigated the performance of two indoor positioning algorithms and compared their performance as a function of RP density and system bandwidth. We also presented mathemati-

cal relations between RP density and achievable MSE and showed how they can be used to ensure the required performance with a given indoor positioning network scenario.

The second part focuses on an analysis tool called MSE profiling developed to benchmark the performance of an indoor positioning system in the presence of UDP conditions.

Performance Benchmarking of TOA-Based UWB Indoor Geolocation Systems Using MSE Profiling

The presence of UDP conditions presents significant challenges for TOA-based indoor geolocation, since it introduces major errors into distance measurements. Therefore, it is critical to characterize the performance of indoor geolocation systems in the presence of UDP conditions. Until now, however, there has been no standard method of performance benchmarking for such cases. Towards that end, we present an analysis tool, known as the MSE Profile, that can aid in this task. We use the MSE Profile to analyze the performance of two TOA-based geolocation algorithms and show how the MSE Profile can be used to gain insight into their performance, in the presence of DME models derived from UWB measurements.

The accuracy of the location estimate can be viewed as a measure of the Quality of Service (QoS) provided by the geolocation system. Different location-based applications will have different requirements for accuracy. In a military or public-safety application (such as keeping track of the locations of fire-fighters or soldiers inside a building), high accuracy is desired. In contrast, lower accuracy might be acceptable for a commercial application (such as inventory control in a warehouse). In such cases, it is essential to be able to answer questions like: "what is the probability of being able to obtain an MSE of 1 m^2 from an algorithm x in any building configuration?" or "what algorithm should be used to obtain an MSE of 0.1 cm^2 in any building configuration?". Answers to such questions will heavily influence the design, operation and performance of indoor geolocation systems. Here, we propose the use of the *MSE Profile* to answer these kinds of questions and illustrate its use with examples.

Although indoor geolocation is a relatively new area, there is a large body of literature on performance analysis of geolocation systems in general. A number of researchers have studied geolocation systems intended primarily for outdoor deployments. A number of different performance metrics have been defined and used. Foy (1976) used the covariance matrix of the position estimation error as a performance metric for the evaluation of Taylor-Series algorithm for geolocation. Torrieri (1984) formally defined and used the circular error probability (CEP), which is a measure of the uncertainty in the location estimate $\hat{x}$, relative to its mean, $E\{\hat{x}\}$. The calculation of the CEP is, in general, quite complicated. This issue can be alleviated by making suitable approximations. However, from a QoS perspective, the most we can say after calculating the CEP is that the estimate is likely to be within $\hat{x}+CEP$ with probability 1/2. The CEP, therefore, will only be of limited use in answering the types of questions given in the previous section. The work of Deng and Fan (2000) and others working in the *E-911* field bears the closest resemblance to our work in the sense that it considers the CDF of the MSE in order to assess the performance of outdoor cellular positioning systems in relation to E-911 requirements outlined by the FCC. However, this cannot be directly applied to our work, as we specifically consider the effect of varying UDP conditions on UWB indoor geolocation system performance. Therefore, to the best of our knowledge, our approach to performance analysis of such systems is unique.

Given the variability of the indoor propagation conditions, it is possible that the distance measurements performed by some of the RPs will be subject to DDP errors, while some will be subject to UDP-

based errors. The DDP/UDP errors can be observed in various combinations. For example, the distance measurements performed by RP-1 in Figure 13 may be subject to UDP-based DME, while the measurements performed by the other RPs may be subject to DDP-based DME; we can denote this combination as *UDDD*. Other combinations can be considered in a similar manner. Since the occurrence of UDP conditions is random, the performance metric used for the location estimate (such as the MSE) will also vary stochastically and depends on the particular combination observed. For the four-RP case shown in Figure 13, it is clear that we will have the following distinct combinations: *UUUU*, *UUUD*, *UUDD*, *UDDD*, and *DDDD*. Each of these combinations can be used to characterize a different type of building environment. The occurrence of each of these combinations will give rise to a certain MSE value in the location estimate. This MSE value will also depend on the specific algorithm used. There may be more than one way to obtain each DDP/UDP combination. If UDP conditions occur with probability P_{udp}, then the overall probability of occurrence of the i-th combination, P_i can be generally expressed as:

$$P_i = \begin{pmatrix} N \\ N_{udp,i} \end{pmatrix} P_{udp}^{N_{udp,i}} (1 - P_{udp})^{N - N_{udp,i}} \tag{43}$$

where N is the total number of RPs (in this case four), and $N_{udp,i}$ is the number of RPs where UDP-based DME is observed. Combining the probabilities, P_i, with the associated MSE values for each combination we can obtain a discrete CDF of the MSE. We call this discrete CDF the *MSE Profile*. In the next section, we will illustrate the use of the MSE Profile with examples.

The algorithms used in this part have already been introduced in the first part. Hence, the results will be presented after introducing the simulation platform.

Simulation Platform

We consider the system scenario in Figure 13 with L = 20 m for each algorithm. A total of 1000 uniformly distributed random sensor locations are simulated for different bandwidth values. Similar to the previous study, we will present our results for bandwidths of 500, 1000, 2000, and 3000 MHz. For each bandwidth value we also simulate different combinations of UDP and DDP-based DMEs for each RP, specifically *UUUU*, *UUUD*, *UUDD*, *UDDD*, *DDDD*. Once a sensor is randomly placed in the simulation area, each RP calculates TOA-based distances to it. The calculated distances are then corrupted with UDP and DDP-based DMEs in accordance with (33). The positioning algorithm is then applied to estimate the sensor location. Based on 1000 random trials, the MSE is calculated for each bandwidth value and the corresponding combinations of UDP and DDP-based DMEs. The probability of each combination is also calculated. For example, take the combination *UUUU* for a bandwidth of 3000 MHz, where two of the RPs are assumed to be far from the sensor, and the other two are assumed to be close. Using the values for $P_{udp,close}$, and $P_{udp,far}$, we can obtain the probability of the combination as 0.0085. The means (denoted by $m_{DDP,w}$ for $\xi_{DDP,w}$ and $m_{UDP,w}$ for $\xi_{UDP,w}$) and standard deviations (denoted by $\sigma^2_{DDP,w}$ for $\xi_{DDP,w}$ and $\sigma^2_{UDP,w}$ for $\xi_{UDP,w}$) are a function of the system bandwidth used to make the TOA-based distance measurements. The parameters for the distributions, as a function of the bandwidth w, are listed in Table 2. As noted by Kanaan & Pahlavan (2004a), the performance of the CN-TOAG algorithm is dependent on the size of the TOA grid, as determined by the the bin size, h, which for the purposes of this study, was varied between 1.25 m down to 0.3125 m for a total of three different values.

Results

The results are shown in Figure 17, Figure 18, Figure 19 and Figure 20. Figure 17 and Figure 18 show the MSE Profiles for the LS and CN-TOAG algorithms respectively. From these plots, we observe that as the bandwidth increases from 500 MHz to 2000 MHz, the range of MSE Profile values gets smaller. This correlates with the findings of Alavi and Pahlavan (2006), where it has been observed that the overall DME goes down over this specific range of bandwidths. Above 2000 MHz, however, the MSE Profile becomes wider as a result of increased probability of UDP conditions (Alavi & Pahlavan, 2006), which increases the overall DME. This, in turn, translates into an increase in the position estimation error for both algorithms. Using the MSE Profile, we can gain insight into the MSE behavior of a given

Figure 17. MSE profile for the LS algorithm

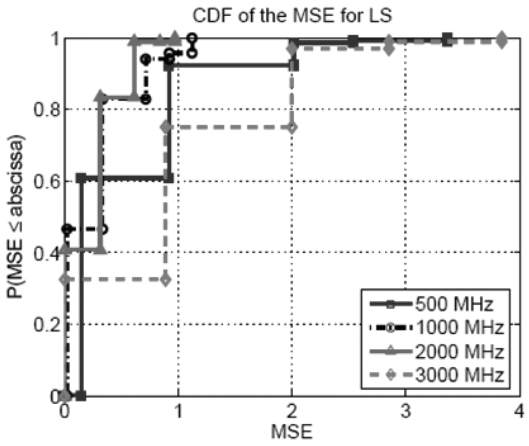

Figure 18. MSE profile for the CN-TOAG algorithm

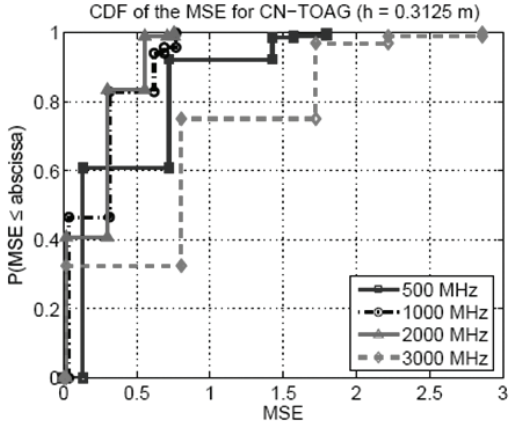

Figure 19. Average MSE comparison: LS vs CN-TOAG

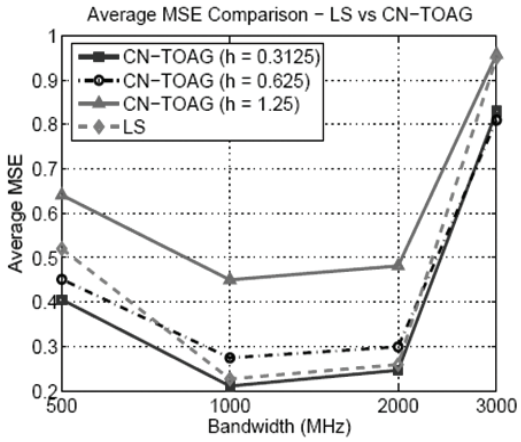

Figure 20. Variance comparison: LS vs CN-TOAG

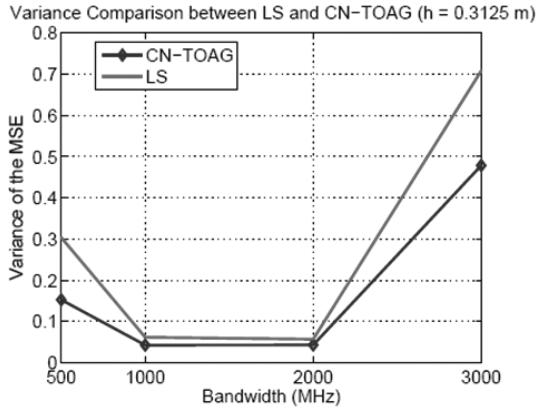

algorithm under varying amounts of UDP (i.e. different building configurations) by calculating the mean and the variance of the MSE for a given bandwidth value. The results of these calculations are shown as a function of bandwidth in Figure 19 and Figure 20. These results clearly indicate that CN-TOAG can outperform LS as long as $h \leq 0.3125$ m. In addition, there appears to be an optimal bandwidth for both algorithms where the average MSE is minimum. Our results indicate that this bandwidth value is 1000 MHz.

Conclusions

In the second part, we proposed the use of the MSE Profile to gauge the performance of any indoor geolocation algorithm under a variety of building conditions. The MSE Profile has been defined as

the CDF of the MSE given the varying severity of UDP conditions across different building environments. We also showed that the MSE Profile can be used for performance benchmarking of different TOA-based indoor geolocation algorithms. We have illustrated its use in analyzing the performance of two algorithms: CN-TOAG and LS. We found that the performance exhibited by both algorithms is in line with previously reported observations on DME behavior. For the scenario and system bandwidths considered, we demonstrated that CN-TOAG can outperform LS as long as the number of points in the grid (as determined by the parameter *h*) is large enough. Specifically, we noted that *h* needs to be about 0.3125 m for the case of a 20m x 20m area in order for CN-TOAG to outperform LS. We also showed that bandwidth of operation of both algorithms needs to be about 1000 MHz in order to guarantee optimal performance across different building configurations.

IMPLEMENTATION AND PRACTICAL ISSUES

Even though no particular emphasis is given to a certain type of technology for the implementation of previous approaches in order to keep the methodology robust and applicable to a broad range of systems, certain aspects of practicality and candidate technologies need to be considered. The success of TOA/TDOA based methods depend primarily on the availability and the quality of RF detection hardware. Although most common systems such as the IEEE 802.11 WLANs and 802.15.4 are not primarily designed for ranging and localization applications, studies exist that show the feasibility of using TOA/TDOA positioning using these systems. The study by Yamasaki et al. (2005) report a positioning accuracy of 2.4m in the 67^{th} percentile with a 802.11b system employing TDOA. The important aspect of AP synchronization is also discussed in this work. Similarly, Duan et al. (2007) report a range estimation error of less than 30cm using the 802.15.4a WPAN standard. The choice of 802.15.4a is also suitable for applications requiring low-power and low cost. Ma et al. (2005) discuss the power aspects of a 802.15.4 based WSN. The UWB PHY layer of 802.15.4a also offers very precise ranging. Hence, 802.15.4a would be a good candidate system for the implementation of TOA based localization using WSNs. However, considering the limited computing power on the 802.15.4 nodes, direct implementation of various algorithms may not be feasible. For this reason, a central computing station (a regular laptop or a PC) with the required technical specs such as memory and CPU speed might be needed to complement the 802.15.4 WSN in order to evaluate the algorithms discussed previously.

CONCLUSION

In this chapter, we presented various aspects of RF and TOA-based localization as applied to WSNs. The challenges of the RF channel have been presented along with their impact on localization algorithms. Particular attention has been given to wireless channel impairments and indoor TOA based systems. The general characteristics of a WSN localization system are discussed and a CRLB expression is also given for the performance of cooperative localization. Methods of remedying underlying wireless channel impairments have been discussed in the context of multipath exploitation along with cooperative localization and UDP detection.

REFERENCES

Akgul, F. O., & Pahlavan, K. (2007). AOA Assisted NLOS Error Mitigation for TOA-based Indoor Positioning Systems. *IEEE MILCOM*. (pp. 1-5). Orlando, FL.

Akyildiz, I., Su, W., Sankarasubramaniam,Y., & Cayirci, E. (2002). A survey on sensor networks, *IEEE Commun. Mag.*, *40*(8), 102-114.

Alavi, B., & Pahlavan, K. (2003). Bandwidth effect of distance error modeling for indoor geolocation. In *IEEE Personal Indoor Mobile Radio Communications Conference (PIMRC)*, *3*, 2198-2202.

Alavi, B., Pahlavan, K., Alsindi, N., & Li, X. (2005). Indoor geolocation distance error modeling with UWB channel measurements. In *IEEE Personal Indoor Mobile Radio Communications Conference (PIMRC)*, *1*, 418-485.

Alavi, B., & Pahlavan, K. (2006). Modeling of the TOA based Distance Measurement Error Using UWB Indoor Radio Measurements. *IEEE Communication Letters*, 10(4), 275-277.

Alavi, B., & Pahlavan, K. (2006). Studying the effect of bandwidth on performance of UWB positioning systems. In *Proceedings of the IEEE Wireless Communications and Networking Conference (WCNC)*, *2*, 884-885.

Alsindi, N., & Pahlavan, K. (2008). Cooperative localization bounds for indoor ultra wideband wireless sensor networks. *EURASIP Journal on Applied Signal Processing (ASP)*,2008. article id 852809. (pp.1-13).

Bahl, P., & Padmanabhan, V.N. (2000). RADAR: An In-Building RF-Based User Location and Tracking system. In *Proc. IEEE INFOCOM 2000*, *2*, 775-784, Tel-Aviv, Israel.

Beauregard, S. (2006). A Helmet-Mounted Pedestrian Dead Reckoning System. In *Proceedings of the 3rd International Forum on Applied Wearable Computing (IFAWC 2006)*. Herzog, O., Kenn, H., Lawo, M., Lukowicz, P., & Troster, G. (Eds.), Bremen, Germany: VDE Verlag. (pp. 79–89).

Blomenhofer, H., Hein, G., Blomenhofer, E., & Werner, W., (1994). Development of a Real-Time DGPS System in the Centimeter Range. *IEEE 1994 Position, Location, and Navigation Symposium*, Las Vegas, NV, (pp. 532–539).

Bulusu, N., Heidemann, J., & Estrin, D. (2000) GPS-less Low-Cost Outdoor Localization for Very Small Devices, *IEEE Personal Communication*, 7(5), 28-34.

Cedervall, M., & Moses, R. L. (1997). Efficient maximum likelihood DOA estimation for signals with known waveforms in the presence of multipath. *IEEE Transactions on Signal Processing*, *45*(3), 808-811.

Chang, C., & Sahai, A. (2004). Estimation Bounds for Localization. *IEEE SECON*. (pp. 415-424).

Chang, C., & Sahai, A. (2006). Cramer-Rao type bounds for localization. *EURASIP Journal on Applied Signal Processing*, *2006*. article id 94287. (pp. 1-13).

Chintalapudi, K., Dhariwal, A., Govindan, R., & Sukhatme, G. (2004). Ad-hoc localization using ranging and sectoring. In *IEEE INFOCOM*, *4*, 2662-2672.

COST 231. (1991). Urban transmission loss models for mobile radio in the 900- and 1,800 MHz bands (Revision 2). COST 231 TD(90)119 Rev. 2, The Hague, The Netherlands.

Cypher, D., Chevrollier, N. Montavont, N., & Golmie, N. (2006). Prevailing over wires in healthcare environments: Benefits and challenges. *IEEE Communications Magazine*, *44*(4l), 56-63.

Dasarathy, B. V. (Ed.) (1991). Nearest Neighbor (NN) Norms: NN Pattern Classification Techniques, ISBN 0-8186-8930-7. *IEEE Computer Society.*

Davidon, W. C. (1968). Variance algorithm for minimization. *Computer Journal*, *10.*

Deng, P., & Fan, P. (2000). An AOA assisted TOA positioning system. In *IEEE WCC-ICCT2000, 2*, 1501-1504.

Denis, B., Keignart, J., & Daniele, N. (2003). Impact of NLOS propagation upon ranging precision in uwb systems. In *IEEE Conference on Ultra Wideband Systems and Technologies*. (pp. 379-383).

Doherty, L., Pister, K. S. J., & Ghaoui, L. E. (2001). Convex Position Estimation in Wireless Sensor Networks, *INFOCOM'01*, *3*, 1655-1663.

Duan, C. D., Orlik, P., Sahinoglu, Z., & Molisch, A. F. (2007). A Non-Coherent 802.15.4a UWB Impulse Radio. *IEEE International Conference on Ultra-Wideband.* (pp. 146-151).

Dumont, L., Fattouche, M., & Morrison, G. (1994). Super-Resolution of Multipath Channels in a Spread Spectrum Location System. *IEE Electronic Letters*, *30*(19), 1583-1584.

FCC-US Federal Communications Commission. (2002). *Revision of part 15 of the commissions rules regarding ultra-wideband transmission systems*. FCC 02-48, First Report & Order.

FCC-US Federal Communications Commission. (1999). *Announcement of Commision Action, FCC Acts to Promote Competition and Public Safety in Enhanced Wireless 911 Services*. [Online]. Available: http://www.fcc.gov/Bureaus/Wireless/News_Releases/1999/nrwl9040.html

Foy, W. H. (1976). Position-location solutions by Taylor-series estimation. *IEEE Trans. Aerospace and Elect. Sys*., *AES-12*(2), 187-194.

Gezici, S., Tian, Z., Giannakis, G. V., Kobaysahi, H., Molisch, A. F., Poor, H. V., & Sahinoglu, Z. (2005). Localization via Ultra-Wideband Radios: A Look at Positioning Aspects for Future Sensor Networks. *IEEE Signal Processing Magazine*. ISSN: 1053-5888, *22*(4), 70-84.

Hata, M. (1980). Empirical formula for propagation loss in land mobile radio services. *IEEE Trans. Veh. Technology*, *29*, 317-325.

Hatami, A., & Pahlavan, K. (2005) A comparative performance evaluation of RSS-based positioning algorithms used in WLAN networks. In *Proceedings of the IEEE Wireless Communications and Networking Conference (WCNC '05), 4*, (pp. 2331–2337), New Orleans, La, USA.

Haykin, S. (2002). *Adaptive Filter Theory – 4th Ed.* Prentice-Hall.

Heidari, M., Akgul, F. O., & Pahlavan, K. (2007a). Identification of the Absence of Direct Path in Indoor Localization System. *IEEE PIMRC 2007.* (pp. 1-6).

Heidari, M., Akgul, F. O., Alsindi, N., & Pahlavan, K. (2007b). Neural Network Assisted Identification of the Absence of the Direct Path in Indoor Localization. *IEEE Globecom 2007.* (pp. 387-392).

Julier, S. J., & Uhlmann, J. K. (1997). A new extension of the Kalman filter to nonlinear systems. *Int. Symp. Aerospace/Defense Sensing, Simul. and Controls.*

JTC (Joint Technical Committee for PCS T1 R1P1.4). (1994). Technical Report on RF Channel Characterization and System Deployment Modeling, JTC (AIR)/94.09.23-065R6.

Kalman, R. E. (1960) A New Approach to Linear Filtering and Prediction Problems. *Transactions of the ASME - Journal of Basic Engineering, 82*, 35-45.

Kanaan, M., & Pahlavan, K. (2004a). Algorithm for TOA-based Indoor Geolocation. *IEE Electronics Letters*, *40*(22).

Kanaan, M., & Pahlavan, K. (2004b). A comparison of wireless geolocation algorithms in the indoor environment. In *IEEE Wireless Communications and Networking Conference (WCNC04)*, *1*, 177-182.

Kanaan M., Akgul, F. O., Alavi, B., & Pahlavan, K. (2006a). A Study of the Effects of Reference Point Density on TOA-Based UWB Indoor Positioning Systems. In the *17th Annual IEEE International Symposium on Personal, Indoor and Mobile Radio Communications, PIMRC*, (pp. 1-5). Finland.

Kanaan, M., Heidari, M., Akgul, F., & Pahlavan, K. (2006b). Technical Aspects of Localization in Indoor Wireless Networks, *Bechtel Telecommunications Technical Journal*, *4*(3).

Kanaan, M., Akgul, F. O., Alavi, B., Pahlavan, K. (2006c). Performance Benchmarking of TOA-Based UWB Indoor Geolocation Systems Using MSE Profiling. In *IEEE 64th Vehicular Technology Conference* (VTC-2006 Fall). (pp. 1-5).

Kim, D., & Langley, R. B. (2000). GPS Ambiguity Resolution and Validation: Methodologies,Trends and Issues. *7th GNSS Workshop-International Symposium on GPS/GNSS*, Seoul, Korea.

Knapp, C., & Carter, G. (1976). The generalized correlation method for estimation of time delay. *IEEE Transactions on Acoustics, Speech and Signal Processing, 24*(4), 320-327.

Krim, H., & Viberg, M. (1996). Two decades of array signal processing research: The parametric approach. *IEEE Signal Processing Magazine*. vol. 13, (pp. 67-94).

Kuchar, A., Tangemann, M., & Bonek, E. (2002). A Real-Time DOA-Based Smart Antenna Processor. *IEEE Transactions on Vehicular Technology*, *51*(6), 1279-1293.

Kumaresan, R., & Tufts, D. W. (1983). Estimating the angles of arrival of multiple plane waves. *IEEE Trans. Aerosp. Electron. Syst*., *AES-19*(1), 134-139.

Larsson, E. G. (2004). Cramer-Rao bound analysis of distributed positioning in sensor networks. *IEEE Signal Processing Letters*, *11*(3), 334-337.

Lee, J. Y., & Scholtz, R.A. (2002). Ranging in a dense multipath environment using an UWB radio link. *IEEE Trans. Select. Areas Commun*., *20*(9), 1677–1683.

Li, J., Halder, B., & Stoica, P. (1995). Computationally efficient angle estimation for signals with known waveforms. *IEEE Transactions on Signal Processing*, 43(9), 2154-2163.

Li, X., & Pahlavan, K. (2004). Super-resolution TOA estimation with diversity for indoor geolocation. *IEEE Trans. on Wireless Communications*, *3*(1), 224-234.

Li, X. (2003). *Super-Resolution TOA Estimation with Diversity Techniques for Indoor Geolocation Applications*. PhD Thesis, WPI.

Ma, J., Min, G., Zhang, Q., Ni, L.M., & Zhu, W. (2005). Localized Low-Power Topology Control Algorithms in IEEE 802.15.4-Based Sensor Networks. *IEEE International Conference on Distributed Computing Systems*. (pp. 27-36).

Merrill, W. M., Newberg, F., Sohrabi, K., Kaiser, W., & Pottie, G. (2003). Collaborative networking requirements for unattended ground sensor systems. *IEEE Aerospace Conference, 5*, 2153-2165.

Motley, A. J. (1988). Radio Coverage in Buildings. *Proc. National Communications Forum*. Chicago. (pp. 1722-1730).

Nerguizian, C., Despins, C., & Affès, C. (2006). Geolocation in Mines With an Impulse Fingerprinting Technique and Neural Networks. *IEEE Transactions on Wireless Communications*, *5*(3).

Niculescu, D., & Nath, B. (2001) Ad Hoc Positioning System (APS), *Global Telecommunications Conference*, *GLOBECOM '01, IEEE*, *5*, 2926-2931.

Okumura Y. et al. (1968). Field Strength and its Variability in VHF and UHF Land-Mobile Radio Service. *Review of the Electrical Communication Laboratory*. Vol. 16, Numbers 9-10.

Oppermann, I., Hamalainen, M., & Linatti, J. (Eds.) (2004). *UWB Theory and Applications*. England: John Wiley and Sons.

Ottersten, B., Viberg, M., & Kailath, T. (1991). Performance analysis of the total least squares ESPRIT algorithm. *IEEE Trans. on Signal Processing*, *39*, 1122-1135.

Pahlavan, K., Krishnamurthy, P., & Beneat, J. (1998). Wideband radio propagation modeling for indoor geolocation applications. *IEEE Communications Magazine*. (pp. 60–65).

Pahlavan, K., Li, X., & Makela, J. (2002). Indoor geolocation science and technology. *IEEE Commun. Mag.*, *40*(2), (pp. 112-118).

Pahlavan, K., & Levesque, A. H. (2005) *Wireless Information Networks - 2nd Edition*. Wiley – Interscience. ISBN: 0-471-72542-0, Hardcover, 722 pages.

Pahlavan, K., Akgul, F. O., Heidari, M., Hatami, A., Elwell, J. M., & Tingley, R. D. (2006). Indoor geolocation in the absence of direct path. *IEEE Wireless Communications*, *13*(6), 50-58.

Pathan, A.-S.K., Choong, S. H., Hyung-Woo, L. (2006). Smartening the environment using wireless sensor networks in a developing country. *The 8th International Conference on Advanced Communication Technology, 1*, 705-709.

Patwari, N., Ash, J. N., Kyperountas, S., Hero, A. O., Moses, R. L., & Correal, N. S. (2005) Locating the nodes: cooperative localization in wireless sensor networks, *IEEE Signal Proc. Mag.*, 22(4), 54-69.

Poling, T. C., & Zatezalo, A. (2002). Interferometric GPS ambiguity resolution, *Journal of Engineering Mathematics*, 43(2-4), 135-151(17).

Priyantha, N. B., Chakraborty, A., & Balakrishnan, H. (2000). The Cricket Location-Support System," *Proc. 6th Ann .lnt1. Conf Mobile Computing and Networking (Mobicom'00)*, ACM Press, (pp. 32-43).

Qi, Y., & Kobayashi, H. (2003). On relation among time delay and signal strength based geolocation methods. In *IEEE Global Telecommunications Conference. GLOBECOM '03.*, *7*, 4079-4083.

Qi, Y., Kobayashi, H., & Suda, H. (2006). Analysis of wireless geolocation in a non-line-of-sight environment. *IEEE Transactions on Wireless Communications*, *5*(3), 672-681.

Qi, Y., Suda, H., & Kobayashi, H. (2004). On time-of arrival positioning in a multipath environment. In *Proc. IEEE 60th Vehicular Technology Conf. (VTC 2004-Fall).* Los Angeles, CA., *5*, 3540–3544.

Randell, C., Djiallis, C., & Muller, H. (2003). Personal position measurement using dead reckoning. In *Proceedings of the Seventh International Symposium on Wearable Computers, IEEE Computer Society.* (pp. 166–173).

Rao, B. D., & Hari, K. V. S. (1989). Performance analysis of root-music. *IEEE Trans*. *ASSP-37*(12), 1939-1949.

Roy, R., & Kailath, T. (1989). ESPRIT-Estimation of Signal Parameters via Rotational Invariance Techniques. *IEEE Transactions on Signal Processing.* 37(7), 984-995.

Röhrig, C., & Spieker, S. (2008). Tracking of Transport Vehicles for Warehouse Management Using a Wireless Sensor Network. *IEEE/RSJ International Conference on Intelligent Robots and Systems*.

Savarese, C., Rabaey, J. M., & Beutel, J. (2001). Locationing in Distributed Ad-Hoc Wireless Sensor Networks, *ICASSP*. (pp. 2037-2040).

Savvides, A., Han, C. C., & Srivastava, M. B. (2001). Dynamic Fine Grained Localization in Ad-Hoc Sensor Networks, *Proceedings of the Fifth International Conference on Mobile Computing and Networking, Mobicom*. (pp. 166-179).

Savvides, A., Garber, W. L., Moses, R. L., & Srivastava, M. B. (2005). An analysis of error inducing parameters in multihop sensor node localization. *IEEE Transactions on Mobile Computing*, *4*(6), 567-577.

Schelkunoff, S. A. (1943). A mathematical theory of linear arrays. *Bell System Technical Journal*, *22*, 80-107.

Schmidt, R. (1986). Multiple emitter location and signal parameter estimation. *IEEE Transactions on Antennas and Propagation*, *AP-34*(3), 276-280.

Schroer, R. (2003). Navigation and landing [A century of powered flight 1903-2003]. IEEE Aerospace and Electronic Systems Magazine, *18*(7), 27-36.

Sohraby, K., Minoli, D., & Znati, T. (2007). Wireless Sensor Networks – Technology, Protocols and Applications. Hoboken, New Jersey: John Wiley & Sons.

Steiner, C., Althaus, F., Troesch, F., & Wittneben, A. (2008). Ultra-Wideband Geo-Regioning: A Novel Clustering and Localization Technique. *EURASIP Journal on Advances in Signal Processing*. article id 296937.

Stoica, P., & Sharman, K. (1990). A Novel Eigenanalysis Method for Direction of Arrival Estimation. *Proc. IEE*, (pp. 19-26).

Stoleru, R., & Stankovic, J. A. (2004). Probability Grid: A location estimation scheme for wireless sensor networks. In *IEEE SECON*. (pp. 430-438).

Tewfik, A. H., & Hong, W. (1992). On the application of uniform linear array bearing estimation techniques to uniform circular arrays. *IEEE Transactions on Signal Processing*, *40*, 1008-1011.

Tingley, R. (2000). *Time-Space Characteristics of Indoor Radio Channel*. PhD Thesis, WPI.

Torrieri, D. (1984). Statistical theory of passive location systems. *IEEE Trans. Aerospace and Elect. Sys. AES-20.*

Van Trees, H. L. (1968). Detection, Estimation and Modulation Theory: Part I. New York: Wiley.

Unbehaun, M. (2002). On the deployment of unlicensed wireless infrastructure. Ph.D. Thesis, Royal Institute of Technology, Department of Signals, Sensors & Systems, Stockholm.

Ward, A., Jones, A., & Hopper, A. (1997). A New Location Technique for the Active Office. In *IEEE Personal Communications, 4*(5), (pp. 42-47).

Wylie, M. P., Holtzman, J. (1996). The non-line of sight problem in mobile location estimation. *5th IEEE International Conference on Universal Personal Communications.* (pp. 827-831).

Yamasaki, R., Ogino, A., Tamaki, T., Uta, T., Matsuzawa, N., & Kato, T. (2005). TDOA location system for IEEE 802.11b WLAN. *IEEE Wireless Communications and Networking Conference,* 4, 2338-2343.

Zaidi, A. S., & Suddle, M. R. (2006). Global Navigation Satellite Systems: A Survey. In *International Conference on Advances in Space Technologies,* (pp. 84-84).

KEY TERMS

Throughout this chapter the words *anchor, reference point, transmitter* have been used interchangeably. Likewise *node, sensor, sensor node, receiver* have been used interchangeably.

ANSI	American National Standards Institute
AOA	Angle-of-Arrival
AP	Access Point
AWGN	Additive White Gaussian Noise
CDF	Cumulative Distribution Function
CEP	Circular Error Probability
CIR	Channel Impulse Response
CN-TOAG	Closest Neighbor Time-of-Arrival
CRLB	Cramer Rao Lower Bound
DDP	Detected Direct Path
DGPS	Differential Global Positioning System
DME	Distance Measurement Error

DOA	Direction-of-Arrival
DP	Direct Path
EKF	Extended Kalman Filter
ESPRIT	Estimation of Signal Parameters via Rotational Invariance Techniques
FCC	Federal Communications Commission
FDP	First Detected Path
FIM	Fisher Information Matrix
GLONASS	GLObal NAvigation Satellite System
GPS	Global Positioning System
IFT	Inverse Fourier Transform
JTC	Joint Technical Committee
LOS	Line-of-Sight
LS	Linear Squares
MAC	Medium Access Control
ML	Maximum Likelihood
MPC	Multipath Component
MSE	Mean Squared Error
MUSIC	Multiple Signal Classification
OLOS	Obstructed-Line-of-Sight
PCS	Personal Communication System
QoS	Quality-of-Service
RF	Radio Frequency
RMS	Root Mean Square
RP	Reference Point
RSS	Received Signal Strength
RT	Ray Tracing
SNR	Signal-to-Noise Ratio
SP	Strongest Path
TDOA	Time-Difference-of-Arrival
TIA	Telecommunication Industry Association
TOA	Time-of-Arrival
UDP	Undetected Direct Path
UKF	Unscented Kalman Filter
ULA	Uniform Linear Array
UWB	Ultra-Wideband
WAAS	Wide Area Augmentation System
WLAN	Wireless Local Area Network
WSN	Wireless Sensor Network